Heliyon 10 (2024) e31755

Contents lists available at ScienceDirect

Heliyon

journal homepage: www.cell.com/heliyon

Research article

Boosting cuckoo optimization algorithm via Gaussian mixture model for optimal power flow problem in a hybrid power system with solar and wind renewable energies

Ali S. Alghamdi [a,*], Mohamed A. Zohdy [b]

[a] Department of Electrical Engineering, College of Engineering, Majmaah University, Al-Majmaah, 11952, Saudi Arabia
[b] Electrical and Computer Engineering Department, Oakland University, Rochester, MI, USA

ARTICLE INFO

Keywords:
Multiobjective OPF
Cuckoo optimization algorithm
Gaussian mixture model
Solar and wind energy
Non-convex cost functions

ABSTRACT

This paper presents a novel approach, the Gaussian Mixture Method-enhanced Cuckoo Optimization Algorithm (GMMCOA), designed to optimize power flow decision parameters, with a specific focus on minimizing fuel cost, emissions, network loss, and voltage deviation. GMMCOA integrates the strengths of COA and GMM while mitigating their individual limitations. While COA offers robust search capabilities, it suffers from initial parameter dependency and the risk of getting trapped in local optima. Conversely, GMM delivers high-speed performance but requires guidance to identify the best solution. By combining these methods, GMMCOA achieves an intelligent approach characterized by reduced parameter dependence and enhanced convergence speed. The effectiveness of GMMCOA is demonstrated through extensive testing on both the IEEE 30-bus and the large-scale 118-bus test systems. Notably, for the 118-bus test system, GMMCOA achieved a minimum cost of $129,534.7529 per hour and $103,382.9225 per hour in cases with and without the consideration of renewable energies, respectively, surpassing outcomes produced by alternative algorithms. Furthermore, the proposed method is benchmarked against the CEC 2017 test functions. Comparative analysis with state-of-the-art algorithms, under consistent conditions, highlights the superior performance of GMMCOA across various optimization functions. Remarkably, GMMCOA consistently outperforms its competitors, as evidenced by simulation results and Friedman examination outcomes. With its remarkable performance across diverse functions, GMMCOA emerges as the preferred choice for solving optimization problems, emphasizing its potential for real-world applications.

1. Introduction

1.1. Background

The operation of electrical energy systems must be economically viable. This means that the cost of production must be lower than the cost of consumption [1,2]. To achieve this, careful planning and execution of energy systems is required [3–5]. This should include energy efficiency, renewable energy sources, and smart grid technologies. The idea of optimal power flow (OPF) is, therefore, fundamental at different levels of planning. As a result of OPF, the energy system can operate efficiently and at the lowest cost possible

* Corresponding author.
E-mail addresses: aalghamdi@mu.edu.sa (A.S. Alghamdi), zohdyma@oakland.edu (M.A. Zohdy).

https://doi.org/10.1016/j.heliyon.2024.e31755
Received 23 September 2023; Received in revised form 21 May 2024; Accepted 21 May 2024
Available online 24 May 2024

[6,7]. In this way, significant savings can be realized in energy production. Additionally, it contributes to identifying design weaknesses and improving the reliability of energy supply [8]. Furthermore, by ensuring that renewable energies have been utilized to their full potential, OPF can diminish the environmental effect of energy production [9].

Various optimizers investigated to the OPF problems. It is a complex problem with static constraints, which has been considered with the development of numerical optimization techniques and computational methods in power system studies [10,11]. Classical techniques for solving OPF problems, such as nonlinear programming [12] and Newton's method [13], have been discussed in various studies. OPF involves multi-objective optimization and is highly nonlinear, so more than one local optimal point is obtained when the problem is resolved. Moreover, due to the need for a criterion for selecting a local minimum as a global minimum, determining the global minimum using classical optimization methods based on the derivative and slope of the line is not suitable [14,15].

1.2. Literature review

OPF is a problem with a non-smooth objective function, non-convex and non-derivative, and this has led to the development and improvement of algorithms to overcome these problems. In the past three decades, intelligent evolutionary methods used to optimize the power flow problems in different networks to dominate the limitations of classical optimizers [16–18]. A brief description of several successful methods is mentioned in the following:

The application of Evaluated Preference Genetic Algorithm (EPGA) for addressing large-scale OPF challenges, considering practical constraints linked to generators, was presented in the study by Ref. [19]. The length of the initial chromosome underwent a stepwise reduction determined by the decomposition level and conformed to the topology of the newly created partition, combined grey wolf optimization (GWO) and differential evolution (DE) [20], these algorithms underwent implementation on the standardized IEEE 30-bus and 118-bus systems across diverse scenarios. The simulation results were rigorously scrutinized and subjected to in-depth analysis. The results obtained showcased the efficacy of the devised algorithms in comparison to other heuristic algorithms contemporaneously documented in the literature. Phasor particle swarm optimization (PPSO) combined with gravitational search algorithm (GSA) [21] that the robustness and efficacy of PPSOGSA for addressing OPF stochastic renewable energy sources (RESs) were evaluated through a comparative study involving 20 well-established metaheuristics. The assessment utilized consistent system data, control variables, and constraints. Statistical attributes of the OPF results were determined through the application of the Monte Carlo method, improved artificial bee colony (IABC) [22] the strategy formulated to tackle multi-objective OPF challenges underwent application on IEEE 30-bus, IEEE 57-bus, and IEEE 300-bus networks. An in-depth comparative analysis with outcomes from alternative algorithms was performed, highlighting the efficacy and superiority of IABC. The optimal scheme derived from the devised model was validated to improve the economic efficiency and stability of the systems.

In the study conducted by Ref. [23], a combination of GA with teaching-learning based optimization (TLBO) was explored. Two performance indicators, specifically fuel cost and algorithm execution time, were utilized for a comprehensive evaluation. The developed algorithm,G-TLBO, integrated the capabilities of GA and TLBO, enabling efficient exploration of both global and local minimum points. Simulation results conclusively demonstrate the enhanced performance of G-TLBO relative to conventional optimization algorithms in terms of fuel cost and algorithm execution time for wind-thermal power systems, modified ABC algorithm [24] the applied method addressed the OPF problem in IEEE 30-bus and IEEE 118-bus networks. A comparative analysis with conventional optimizers assessed its performance and operation. Simulation results affirmed the efficacy of the proposed approach, glow-worm swarm optimization (GSO) [25] the algorithms' efficacy was evaluated on IEEE 30-bus and practical Indian 75-bus systems for cost minimization and on IEEE 30-bus network for cost and emission minimization. Results from both networks were compared, assessing PSO and GSO based on various parameters.

Several studies have explored the application of Fitness-Distance Balance (FDB) selection methods in meta-heuristic search algorithms, especially within the realm of power system optimization integrating renewable energy sources [26–28]. For instance, research has investigated FDB-based adaptive guided differential evolution (FDBAGDE) [27] and the Lévy roulette FDB-coyote optimization algorithm (LRFDBCOA) [28] for addressing security-constrained optimal power flow (SCOPF) problems incorporating RESs. These studies have highlighted how integrating FDB principles can bolster the balance between exploration and exploitation within algorithms, thus driving advancements in optimization methodologies.

The multi-objective dynamic optimal power flow (MODOPF) problem [29] was addressed through a hybrid approach that combined the non-dominated sorting genetic algorithm II (NSGA-II) with a fuzzy satisfaction-maximizing method. NSGA-II determined the Pareto frontier, and the fuzzy satisfaction-maximizing method was selected as the strategy. Illustrative cases in various scenarios, utilizing an IEEE 6-units\30-nodes network, were conducted to validate the proposed model, solution process, and the advantages introduced by demand response (DR) in the power system, Harris hawks optimization (HHO) methodology [30] that this paper optimized power system control variables by considering fuel cost, real power loss, and environmental emissions as single and multi-objective functions. Conflicting multi-objective functions were resolved using weighted sums with a no-preference method. The method was implemented in MATLAB using an IEEE 30-bus network, demonstrating its efficacy on selective objectives. Results were compared with other Artificial Intelligence (AI) techniques, additionally, the study on distributed generation (DG) placement indicated reductions of 9.8355 % in system losses and 26.2 % in emissions.

The turbulent flow water-based optimizer (TFWO) [9] underwent testing on the IEEE 30-bus and 57-bus networks, encompassing a total of 17 cases. An additional four cases were examined on large-scale test systems, showcasing the scalability of the methodology. Evaluation of the TFWO's effectiveness and robustness involved a thorough comparison of simulation results, convergence rates, and statistical indices against other recent methods. Conclusions from the study highlight TFWO's efficiency, effectiveness, robustness, and superiority in solving OPF. It demonstrated better convergence rates and achieved a reduction in the range of 4.6–33.12 % for the

large-scale network. TFWO led to a more competitive solution with significant improvements in techno-economic aspects.

A modified version of PSOGSA integrated with chaotic maps (CPSOGSA) was introduced in this paper [31]. Composite benchmark test functions were applied, and OPF problems with stochastic wind power and Flexible Alternating Current Transmission System (FACTS) devices were solved. The effectiveness of CPSOGSA compared to other methods was illustrated through numerical studies. Superiority and robustness in solving OPF were demonstrated by the Wilcoxon signed-rank test. Case studies highlighted the potential of CPSOGSA in effectively addressing these challenges, coronavirus herd immunity optimizer (CHIO) [32] that several scenarios were examined to validate the problem-solving capability of the defined optimization model. The model's proficiency in problem-solving was confirmed through various scenarios. The multi-objective problem was transformed into a normalized one-objective issue using a weighted sum approach employing the Analytical Hierarchy Process (AHP). The Technique for Order Preference by Similarity to Ideal Solution (TOPSIS) was introduced to identify the optimal value of Pareto alternatives. The results indicated that CHIO outperformed other methods in solving the problem. Applied to 30, 57, and 118-bus test systems, the algorithm's results were compared with existing literature, the OPF problem in power systems was addressed through the utilization of a novel Sine-Cosine algorithm.

Additionally, a power flow-based hydro-thermal-wind scheduling approach for hybrid power systems was developed, employing the sine-cosine algorithm (SCA) [33,34], slime mould algorithm (SMA) [35] the performance of the SMA was assessed on the IEEE 30-bus and Algerian DZA 114-bus networks. Comparative analysis involved four optimization algorithms, results demonstrated the SMA's superiority across diverse function landscapes, consistently ranking first among the compared algorithms, antlion optimization (ALO) [36] the OPF problem integrated real-time measurements and probabilistic wind speed models for anticipated active power generation from WT. Evaluation criteria included operational costs, voltage profile, and network-wide transmission power losses. The validation was conducted on the modified IEEE 30-bus network, cross entropy-cuckoo search algorithm (CE-CSA) [37] that CE-CSA efficiently solved OPF, considering Renewable Energy Sources (RESs) and controllable loads across various stochastic scenarios in a benchmark system to minimize total operation costs. Its performance was compared with state-of-the-art hybrid methods, demonstrating superior results. Comparative analyses, including the Analysis of Variance (ANOVA) test, Tukey Honestly Significant Difference test, and Wilcoxon Sign Rank test, validated the effectiveness of the proposed algorithm over various optimization techniques, a new developed GWO [38], DGWO, for efficient OPF. DGWO increased population diversity through random mutation, enhanced exploitation by updating positions around the best solution, and employed adaptive operators for balanced exploration and exploitation. DGWO demonstrated superior effectiveness over other well-known meta-heuristic techniques, modified honeybee mating optimization (MHBMO) [39], MHBMO, as demonstrated by simulation results, outperformed the original HBMO and other methods in the literature, social spider optimization (SSO) [40], the [40] introduced the Novel Improved SSO (NISSO) algorithm for independently optimizing fuel cost, L index, voltage deviation, polluted emission, and power loss in OPF. NISSO incorporates three modifications to enhance solution quality and accelerate convergence compared to conventional SSO.

Multi-objective mayfly algorithm (MOMA) [41], was conducted in normal and contingency conditions. Fuzzy Decision-Making determined optimal compromise solutions, and a preference selection index assessed computational efficiency. Novel Line Stability Index (NLSI) and Voltage Collapse Proximity Index (VCPI) achieved the best system performance, simulation time transmission loss, and minimizing generation costs. MOMA outperformed other algorithms, providing the lowest system cost and loss, bird swarm algorithm (BSA) [42], the BSA consistently outperformed other metaheuristic algorithms in achieving accurate and stable results. In case study 1, this approach demonstrated superiority in solving OPF, meeting all constraints and achieving a best generation cost of 863.121 $$/h. Additionally, in case study 2, the BSA outperformed other methods, achieving a minimum electricity cost of 890.728 $$/h, especially when considering the imposition of a carbon tax, two-point estimate method (2PEM) [43], five diverse methods were employed for solving MOOPF using 2PEM for comparison. The results underscored the superiority of 2PEM in attaining optimal outcomes. Adaptive group search optimization (AGSO) [44], AGSO's effectiveness in solving nonlinear and nonconvex problems was validated through simulation studies on benchmark test cases and IEEE standard 30-bus and 57-bus networks, affirming its accuracy, modified bacteria foraging algorithm (MBFA) [45], after extensive testing, MBFA optimization demonstrated superiority over hybrid method and GA, ensuring the voltage stability and cost-effectiveness of the IEEE30-bus network, effective cuckoo search algorithm (ECSA) [46], comparisons show ECSA's superior effectiveness in minimizing the system's operational cost. Additionally, considering uncertainty and certainty of wind and solar, node 30 with higher loss sensitivity factor is identified as more suitable for photovoltaic power plants placement than node 3. Consequently, integrating ECSA with the second solution method is recommended for OPF in the integrated wind-solar-hydro-thermal power system.

The Jaya algorithm [47] demonstrated superior optimality and feasibility compared to various stochastic algorithms, as evidenced by its optimal solution. Remarkably, DG placement further improved the solutions, modified JAYA (MJAYA) [48] the effectiveness of MJAYA was demonstrated by its application to two electrical networks (IEEE 30-bus and IEEE 118-bus). Results from various scenarios using MJAYA were compared with other published methods, revealing its superiority across different complexities, circulatory system-based optimization (CSBO) [49] and Gaussian Bare-bones Levy CSBO (GBLCSBO) [50], the optimization outcomes, encompassing OPF problems and diverse test functions, revealed the strength, robustness, and competitive performance of CSBO and GBLCSBO algorithms across various modern optimization methods. The results underscored GBLCSBO's high potential in effectively addressing OPF problems.

Wind power-integrated OPF solutions were first proposed in Ref. [51]. In Ref. [52], a multi-objective GSO successfully solved the optimization problem on modified IEEE 30 and 300 bus test systems, incorporating wind farms at different buses. The simulation results affirmed the suitability and effectiveness of the MOOPF problem. In Ref. [53], a hybrid PSO-GWO was proposed, and its performance and robustness in solving OPF were evaluated by comparing results with five other metaheuristics. Using the same test system, system constraints, and control variables, simulation results verified the efficiency of PSO-GWO, positioning it as a viable choice for OPF problem solutions. Voltage stability-constrained OPF solutions were introduced in Ref. [54], where the implemented

technology effectively prevented potential voltage collapse in typical networks, enhancing system stability and ensuring a sufficient stability margin for increased security. Multi-objective DE methods were tested on enhanced IEEE 30-bus and 57-bus electrical networks in Refs. [55,56], and results were compared with NSGA-II, SPEA 2, and pareto DE.

In [57,58], the performance of Invasive Weed Optimization (IWO) with chaos (CIWOs) was assessed on the IEEE 30-bus electrical network across various objective functions. Experimental findings indicated that the CIWO technologies exhibit significant promise as efficient and powerful optimization tools for electrical networks. In Ref. [59], a Multi-objective Evolutionary Algorithm (MOEA) incorporated the effect of intermittence from plug-in electric vehicles (PEVs), PV, and wind integration into optimal cost analysis. Uncertainties related to these systems were modeled using Probability Density Functions (PDFs), and Monte Carlo Simulations (MCSs) calculated their uncertainty cost. Comparative examination was performed using the ANOVA test on standard IEEE 30, 57, and 118-bus electrical networks with various cases.

The hybrid Artificial Physics Optimization (APO) and Particle Swarm Optimization (PSO) method (HPSO-APO) [60] demonstrated superior efficiency and robustness compared to standard techniques in acquiring diverse Pareto optimal solutions. This highlights its effectiveness in addressing security-constrained Multi-Objective Optimal Power Flow (MO-SCOPF) challenges within large interconnected power systems integrating wind and thermal generators.

The Improved Strength Pareto Evolutionary Algorithm (ISPEA2) [61] showcased its capability to generate evenly distributed Pareto optimal solutions for MOOPF. Its superiority was validated through comparative analysis with other algorithms, affirming its effectiveness. The Chaotic Bonobo Optimizer (CBO) [62] addressed three distinct objectives: minimizing total operating cost, power losses, and emissions, including a carbon tax in the objective function to reduce carbon emissions. Verification on adapted IEEE-30 and IEEE-57 bus electrical networks affirmed the superiority and effectiveness of CBO in attaining optimal solutions, particularly in OPF involving stochastic Renewable Energy Sources (RESs).

The Modified Moth Swarm Algorithm (MMSA) [63] targeted three objectives: minimizing operating cost, improving voltage profile, and reducing transmission losses. Comparative assessments validated the efficiency and superiority of MMSA in addressing these objectives.

The BAT Optimizer [64] was implemented and assessed on developed IEEE 30-bus and 5-bus electrical networks, both with and without UPFC. Comparative analysis with Genetic Algorithms (GA) showcased the efficacy of the BAT approach in optimizing electrical network performance. The Multi-Objective Electromagnetism-Like Optimizer (MOELA) [65] demonstrated feasibility using the IEEE 30-bus electrical network. Comparative numerical analysis with various optimizers documented its efficacy over alternative methods. In Ref. [66], the application of DE and PSO (DEPSO) algorithms to optimize the OPF of electrical networks with controllable wind-photovoltaic energy systems was explored. Simulations were conducted on three distinct test systems: the IEEE 30-bus, IEEE 57-bus, and a real-world 62-bus Indian utility electrical network. The aim was to assess the effectiveness of the Interior Search Algorithm (ISA) [67] in addressing OPF problems. Comparative analysis with alternative techniques demonstrated the utility of ISA in solving Multi-Objective OPF (MOOPF) problems.

In the context of surrogate-assisted Multi-Objective Probabilistic OPF (POPF) [68], the study addressed the MOOPF problem using multi-objective DE. It considered factors such as residential load, ambient temperature, solar irradiation, historical data, and electric vehicle (EV) travel distance in the low voltage distribution system, illustrating the potential benefits of the devised method.

Expected Security Cost Dynamic OPF (ESCDOPF) [69] was implemented to substantiate the proposed model and solution procedure. Illustrative scenarios across different conditions were executed on an IEEE-30 bus electrical network, indicating that the implemented DE fulfilled all model constraints while yielding cost reductions through the integration of solar and flexible resources into the electrical network. Enhanced Colliding Bodies Optimization (ICBO) [70] showcased its efficacy in addressing various OPF problems, outperforming algorithms documented in the literature. Multi-Objective Adaptive Group Search Optimization (MOALO) [71] demonstrated adaptability and efficiency across diverse electrical networks, particularly in handling large-scale systems. Comparative analyses with other documented algorithms validated its effectiveness.

A new and improved Adaptive Differential Evolution (DE) [72] was proposed and verified by its application to OPF on a modified IEEE 30-bus electrical network. Through simulation results, it was confirmed that the proposed DE provides an effective and viable alternative for addressing OPF, especially in systems integrated with stochastic solar energy and wind energy alongside thermal generators. In Ref. [73] the AC OPF with thermal-tidal-solar-wind energy sources was addressed through the utilization of the symbiotic organisms search algorithm (SOS) the simulation results of SOS underwent comparison with results from other algorithms, including the harmony search (HS), and GSA, imperialist competitive algorithm (ICA) and backtracking search optimization (BSO), etc.

In summary, a wide array of optimization techniques has been explored and applied to address the challenges of OPF in power systems. These studies have demonstrated the effectiveness and superiority of various algorithms in achieving optimal solutions, thereby contributing to advancements in power system optimization methodologies.

1.3. Motivation and contribution

The Cuckoo Optimization Algorithm (COA), initially introduced in 2011, has emerged as a versatile optimization technique with widespread applications [74]. Inspired by the intriguing behavior of cuckoos in nature, this algorithm has garnered significant attention across various domains due to its effectiveness in solving complex optimization problems. Notably, researchers have utilized

COA to address intricate challenges such as crack detection in cantilever Euler-Bernoulli beams [75], optimization of combined heat and power (CHP) plants [76], and efficient data clustering [77]. Moreover, COA has been integrated into load balancing strategies to effectively manage energy consumption in cloud computing platforms [78].

The appeal of the COA lies in its capacity to address intricate optimization problems with simplicity and ease of implementation. Its emulation of cuckoo behavior facilitates robust exploration and exploitation of solution spaces, rendering it well-suited for the diverse optimization needs of modern systems. This study leverages the strengths of COA to tackle the OPF issue in hybrid power systems. Despite its proven effectiveness and adaptability, COA faces challenges navigating complex, non-smooth, and non-convex OPF problems coupled with the variability introduced by renewable energy sources such as solar and wind; hence, it may become trapped in local optima. To overcome these limitations, we introduce the Gaussian Mixture Method (GMM) as a complementary technique to enhance COA's capabilities and effectively address various OPF problems. Integrating GMM with COA mitigates the risk of converging to suboptimal solutions and improves the algorithm's ability to explore the solution space. This strategic amalgamation empowers the proposed approach to efficiently handle the complexities of OPF problems, leading to enhanced performance and reliability in hybrid power systems. This study represents a synergistic fusion of COA and GMM, capitalizing on their respective strengths to overcome OPF's challenges in hybrid power systems. Through meticulous experimentation and evaluation, this paper demonstrates the efficacy of the proposed method in delivering superior solutions to a range of OPF problems, thereby advancing state-of-the-art power system optimization.

1.4. Paper structure

The rest of the study is structured as follows: Section 2 defines the OPF optimization formulation. Section 3 elaborates on the optimization process of GMMCOA. In Section 4, GMMCOA is applied to the IEEE 30-bus system with various OPF functions, and the simulation solutions are analyzed. The benchmarking of the proposed method is conducted in Section 5, followed by the general conclusions presented in Section 6.

2. Problem statement

2.1. Objective function

The aim of using OPF is manifold. It can be used for finding the best operating point at which the cost, pollution level, and power loss are minimized or for other objectives and, at the same time, to observe the operating limitations of the system [79,80]. In terms of power systems, an OPF problem majorly is formulated based on control parameters that is either continuous or discrete. Also, the nature of an OPF problem is often non-convex and nonlinear, with numerous variables to discover. So, an OPF problem purposes at finding the best status of electrical networks at different levels subject to many operation boundaries. An OPF's objective is to find the system's operating status, including the amount of power passing through the lines, bus voltage, and current on the lines.

Incorporating solar and wind renewable energies into the optimal power flow (OPF) problem presents significant challenges due to their intermittent nature, leading to uncertainty in generation forecasts. This unpredictability is further compounded by spatial and temporal variability, necessitating sophisticated modeling techniques for accurate integration. Moreover, with the restructuring of power networks involving the addition of new devices, power storage solutions, and changes in energy market dynamics, the OPF problem faces additional complexities [81,82]. Grid stability concerns and the imperative for optimal utilization add layers of intricacy to the optimization process. Consequently, addressing these multifaceted challenges requires the deployment of advanced optimization methods capable of precisely modeling renewable energy dynamics and efficiently optimizing power flow. By doing so, we can pave the way for a smoother transition towards sustainable energy systems.

The main objective functions of the hybrid OPF problem are given below.

2.1.1. The cost function of wind turbine (WT)

Thanks to the significant benefits of wind energy, such as its low cost and availability, it has found its standing in power systems. Equation (1) mathematically expresses the cost function for the output power of the ith WT ($C_{d,w,i}$) [83]:

$$C_{d,w,i} = d_{w,i} P_{w,i} \tag{1}$$

where $P_{w,i}$ and $d_{w,i}$ indicate the scheduled wind power and direct cost coefficient related of the ith WT, respectively. Suppose the wind output energy is not distributed among the customers according to the predetermined schedule. In that case, the operators should pay penalty costs, including two types of costs: underestimation ($C_{ue,w,i}$) and overestimation ($C_{oe,w,i}$). The former refers to the cost that needs to be paid when only part of the generation power of WT has been utilized. At the same time, the latter represents the cost imposed by purchasing power from storage or demand removal (reduction). Equations (2) and (3) models the two costs [84]:

$$C_{oe,w,i} = K_{oe,w,i} \int_0^{P_{w,i}} \left(P_{w,i} - P_i\right) f(P_i) dP_i \tag{2}$$

$$C_{ue,w,i} = K_{ue,w,i} \int_{P_{w,i}}^{P_{w,r,i}} (P_i - P_{w,i}) f(P_i) dP_i \tag{3}$$

i is an integer ranging from 1 to nw (the number of wind sources), and $f(P_i)$ is the probability density function (PDF) of energy generation by WTs (P_i), $P_{w,r,i}$ rated output power of the ith WT, $K_{oe,w,i}$ shows the reserve cost factor of the ith WT, $K_{ue,w,i}$ shows the penalty cost factor of the ith WT.

The overall cost ($\int_{i=1}^{n_w} COS\ T_{w,i}$) is given in Equation (4) [84].

$$\int_{i=1}^{n_w} COS\ T_{w,i} = \sum_{i=1}^{n_w} C_{d,w,i} + C_{oe,w,i} + C_{ue,w,i} \tag{4}$$

The intermittent speed of wind (Vw) is expressed using the Weibull PDF, $f(Vw)$ (the probability of wind speed) and cumulative distribution function (CDF), $F(Vw)$ in Equations (5) and (6), respectively [83]:

$$f(V_w) = \frac{K}{C}\left(\frac{V_w}{C}\right)^{K-1} e^{-\left(\frac{V_w}{C}\right)^k}, V_w > 0 \tag{5}$$

$$F(V_w) = 1 - e^{-\left(\frac{V_w}{C}\right)^k}, V_w > 0 \tag{6}$$

So, the output power (P_w) from WT for different speeds of wind (V_w) can be calculated using Equation (7) [84]:

$$P_w(V_w) = \begin{cases} 0, V_w < V_{w,in}, V_w > V_{w,out} \\ \frac{P_{w,r}}{V_{w,r} - V_{w,in}} V_w - \frac{V_{w,in} P_{w,r}}{V_{w,r} - V_{w,in}}, V_{w,in} \le V_w \le V_{w,r} \\ P_{w,r}, V_{w,r} \le V_w \le V_{w,out} \end{cases} \tag{7}$$

Here, $V_{w,r}$, and V_w are the rated and current speed of the wind, $V_{w,\text{ in}}$, and $V_{w,\ out}$ denote the cut-in and cut-out speed of the wind, and C and K are the scale and shape variables related to the Weibull PDF.

2.1.2. The cost function of photovoltaics

Photovoltaics (PV), similar to WTs, is among the popular source of green energy, which imposes less cost and is freely accessible to be employed in power systems for energy generation purposes. The output energy or power (P_i) of a PV relies on irradiation and temperature, which vary significantly over time. Equations (8)–(10) present the PV output reserve power cost ($C_{oe,pv,i}$) and penalty cost ($C_{ue,pv,i}$) [83]:

$$C_{d,pv,i} = d_{pv,i} P_{pv,i} \tag{8}$$

$$C_{ue,pv,i} = K_{ue,pv,i} \int_{P_{pv,i}}^{P_{pv,r,i}} (P_i - P_{pv,i}) f(P_i) dP_i \tag{9}$$

$$C_{oe,pv,i} = K_{oe,pv,i} \int_{0}^{P_{pv,i}} (P_{pv,i} - P_i) f(P_i) dP_i \tag{10}$$

Where i is a natural number varying from 1 to nv(the number of PV sources), $C_{d,pv,i}$ is the direct cost pertaining to i-th PV with the scheduled power ($P_{pv,i}$) and the direct cost coefficient ($d_{pv,i}$), the rated output power ($P_{pv,r,i}$), and $f(P_i)$ is the PDF of energy generation by the PV system. The overall cost ($\int_{i=1}^{n_v} COS\ T_{pv,i}$) imposed by a PV system is shown in Equation (11) [84]:

$$\int_{i=1}^{n_v} COS\ T_{pv,i} = \sum_{i=1}^{n_v} C_{d,pv,i} + C_{ue,pv,i} + C_{oe,pv,i} \tag{11}$$

We can also estimate the PDF of energy generation by the ith PV according to the following steps:

There is a strong correlation between irradiation and the energy generation of PV cells. Modeling of the PDF of irradiance $f(R)$ is given using the beta distribution as given in Equation (12) [83]:

$$f(R) = \frac{\Gamma(\alpha+\beta)}{\Gamma(\alpha)\Gamma(\beta)} R^{\alpha-1}(1-R)^{\beta} \tag{12}$$

In this equation, $\Gamma(.)$ denotes the gamma function, where α and β show variables of the beta distribution, and R shows the irradiation.

Equation (13) shows how power generation by a PV system depends on irradiation [83]:

$$P_{PV}(R) = \begin{cases} P_{PV,r}\left(\dfrac{R^2}{R_{STD}R_C}\right), 0 < R \le R_C \\ P_{PV,r}\dfrac{R}{R_{STD}}, R_C < R \le R_{STD} \\ P_{PV,r}, R > R_{STD} \end{cases} \tag{13}$$

R_C and R_{STD} express the irradiance (W/m^2). Radiation is commonly assumed to be 150 W/m2, considered 100 W/m^2.

2.1.3. The conventional quadratic cost function of fuel

The primary function in formulating the OPF concerns the fuel cost, which has been calculated via a quadratic polynomial function as expressed in Equation (14) [83,85]:

$$J = \sum_{i=1}^{nG} f_i(P_{Gi}) = \sum_{i=1}^{nG} \left(\alpha_i + b_i P_{Gi} + c_i P_{Gi}^2\right) \tag{14}$$

$i = 1, 2, \ldots, nG$ denotes the ith power unit, and a_i, b_i, and c_i show coefficients of the cost related to the ith unit, $f_i(P_{Gi})$ the cost of i-th unit. Also, P_{Gi} shows the generation of the ith unit.

2.1.4. The piecewise quadratic cost function of fuel

The fuel cost of a unit is shown via a piecewise quadratic function in Equations (15) and (16):

$$J = \sum_{i=1}^{nG} f_i(P_{Gi}) \tag{15}$$

where

$$f_i(P_{Gi}) = \sum_{k=1}^{n_f} \alpha_{i,k} + b_{i,k} P_{Gi} + c_{i,k} P_{Gi}^2 \tag{16}$$

Equation (16) shows quadratic parts of the cost [70], in which n_f is the number of the fuel alternatives of generator i, and $a_{i,k}$, $b_{i,k}$, and $c_{i,k}$ express cost coefficients of the generator for the kth fuel alternative.

2.1.5. The non-convex cost function of fuel considering valve point effects (VPEs)

A unit's cost function has been modeled as a convex function constrained by the turbine valves' operation. To accurately model the cost of a generator, the valve point effect needs to be taken into account using Equation (17) [83]:

$$J = \sum_{i=1}^{nG} \alpha_i + b_i P_{Gi} + c_i P_{Gi}^2 + \left| e_i \sin\left(f_i\left(P_{Gi}^{\min} - P_{Gi}\right)\right)\right| \tag{17}$$

Here, e_i and f_i are the cost coefficients related to the valve point for generator i.

2.1.6. The cost function of pollutant

As conventional power-generating units work based on fossil fuels, significant amounts of pollutant gases are emitted into the air. Equation (18) provides modeling of these emissions for NO_x and SO_x gases [83]:

$$E = \sum_{i=1}^{nG} f_{Ei}(P_{Gi}) = \sum_{i=1}^{nG} \left(\alpha_i + \beta_i P_{Gi} + \gamma_i P_{Gi}^2 + \xi_i \exp(\theta_i P_{Gi})\right) \tag{18}$$

In this equation, θ_i, β_i, α_i, and ξ_i denote the emission coefficients related to generating unit i.

2.1.7. The cost function of power losses

The cost function related to optimizing losses (P_{Loss}) on the lines is expressed as Equation (19) [83]:

$$P_{Loss} = \sum_{i=1}^{N_l} \sum_{\substack{j=1 \\ j \neq i}}^{N_l} G_{ij} V_i^2 + B_{ij} V_j^2 - 2 V_i V_j \cos \delta_{ij} \tag{19}$$

where, N_l shows the number of network lines, B_{ij} and G_{ij} show the imaginary and real sections of the element on row i and column j of the admittance matrix, δ_{ij} represents the voltage phase angle difference between buses i and j, and V_i shows the voltage of bus i.

2.1.8. The cost function of voltage deviation (VD)

The voltage of buses should be preserved within the allowable boundary, and any deviation from the default magnitude of 1 p.u. is formulated in Equation (20) [83]:

$$VD = \sum_{i=1}^{n_{PQ}} |VL_i - 1.0| \tag{20}$$

Here, n_{PQ} shows the number of buses on which a load is placed, and VL_i represents the voltage magnitude of bar bus i.

2.2. Constraints

Many constraints must be observed when formulating an OPF problem, some of which are introduced as follows [83].

- Active-reactive power balance

$$P_{Gi} - P_{Di} = \sum_{j=1}^{n} V_i V_j \left[B_{ij} * \sin\left(\delta_{ij}\right) + G_{ij} * \cos\left(\delta_{ij}\right) \right], i = 1, \ldots, n \tag{21}$$

$$Q_{Gi} - Q_{Di} = \sum_{j=1}^{n} V_i V_j \left[- B_{ij} * \cos\left(\delta_{ij}\right) + G_{ij} * \sin\left(\delta_{ij}\right) \right], i = 1, \ldots, n \tag{22}$$

In Equations (21) and (22), n shows the number of buses, Q_{Gi} and P_{Gi} show reactive and real power of generator ith, while P_{Di} and Q_{Di} are similar quantities related to the load located on bus i.

- Voltage magnitude

$$V_i^{\min} \leq V_i \leq V_i^{\max}, i = 1, 2, \ldots, n_G \tag{23}$$

$V_i^{\min}$ and $V_i^{\max}$ denote the minimum and maximum boundaries of voltage magnitude of bus i in Equation (23).

- Generating power for $i = 1, 2, \ldots, n_G$.

$$P_{Gi}^{\min} \leq P_{Gi} \leq P_{Gi}^{\max} \tag{24}$$

$$Q_{Gi}^{\min} \leq Q_{Gi} \leq Q_{Gi}^{\max} \tag{25}$$

In Equations (24) and (25), $P_{Gi}^{\min}$ and $P_{Gi}^{\max}$ define the limits on active power produced by unit i, while $Q_{Gi}^{\min}$ and $Q_{Gi}^{\max}$ represent the limits on reactive power of that unit.

- Tap-changers limits

$$T_i^{\min} \leq T_i \leq T_i^{\max}, i = 1, 2, \ldots, N_{tab} \tag{26}$$

where, in Equation (26) $T_i^{\min}$ and $T_i^{\max}$ represent the limits on tap-changer of transformer i, and N_{tab} shows the number of tap-changers.

- Shunt compensator limits (Equation (27))

$$Q_{c,i}^{\min} \leq Q_{c,i} \leq Q_{c,i}^{\max}, i = 1, 2, \ldots, N_{cap} \tag{27}$$

Here, $Q_{c,i}^{\min}$ and $Q_{c,i}^{\max}$ represent the limits on shunt compensator i, and N_{cap} is the number of capacitors.

- Loading conditions of lines

$$|S_i| \le S_i^{\max}, i = 1, 2, \ldots, N_l \tag{28}$$

In Equation (28), $S_i^{\max}$ shows a transmission line's maximum mega-volt-ampere (MVA) capacity, and N_l is the number of transmission lines.

- The real power output of a WT (Equation (29))

$$0 \le P_{w,i} \le P_{w,r,i} \tag{29}$$

- The generation power of a PV (Equation (30))

$$0 \le P_{pv,i} \le P_{pv,r,i} \tag{30}$$

2.3. Constraints handling: considering of the state variables constraints in the OPF's objective function

In the examination of the infringement of penalty function constraints, the fundamental objective function incorporated the subsequent term. A penalty factor, *PF*, is integrated to check the infringement of constraints as formulated in Equation (31) [83,86]:

$$J = \sum_{i=1}^{nG} f_i(P_{Gi}) + PF = \sum_{i=1}^{nG} f_i(P_{Gi}) + \lambda_P \left(P_{G1} - P_{G1}^{\lim}\right)^2 + \lambda_Q \sum_{i=1}^{n_G} \left(Q_{Gi} - Q_{Gi}^{\lim}\right)^2 + \lambda_V \sum_{i=1}^{NPQ} \left(VL_i - VL_i^{\lim}\right)^2 + \lambda_S \sum_{i=1}^{N_l} \left(S_{li} - S_{li}^{\lim}\right)^2 \tag{31}$$

where λ_Q, λ_V, λ_P, and λ_S indicate the penalty coefficients, and x^{lim} is an additional parameter expressed in Equation (32):

$$x^{\lim} = \begin{cases} x; & x^{\min} \le x \le x^{\max} \\ x^{\min}; & x \le x^{\min} \\ x^{\max}; & x \ge x^{\max} \end{cases} \tag{32}$$

3. Cuckoo optimization algorithm

As previously mentioned, COA was introduced over a decade ago [74]. The algorithm is formed based on cuckoo laying and Levy flight. COA starts with a random initial population with several eggs like its counterpart. Then, the eggs are placed in the nests of other birds to be hatched after a specific period. Cuckoos do not attempt to hatch their eggs, which is performed with other birds' help. However, this action is considered a fantastic approach to surviving their generation.

Nevertheless, if the host recognizes the eggs as dissimilar, the bird will more likely destroy them. The process evolves; cuckoos learn to lay eggs themselves, and the host learns to identify them as not their own correctly. In cases the number of eggs maintained in the host nest is large, the nest (the parameter to be optimized by the COA) is more trustable, and cuckoos can count on that as an excellent place to put their eggs. The steps of implementation of the COA are described as follows.

- Initial population

First, the problem parameters are structured as a *habitat* array. The next D of this array is a $1 \times D$ dimension array that includes the current position X_i of the member i-th and is shown by Equation (33):

$$X_i = [x_1, x_2, \ldots, x_D] \tag{33}$$

Then the profit (suitability) function *f*(*Habitat* or X_i) is assessed to achieve the suitability of the present habitat using Equation (34):

$$f(X_i) = f([x_1, x_2, \ldots, x_D]) \tag{34}$$

Another $Npop \times D$ dimension habitat matrix is formed to start the optimization procedure, and eggs are randomly assigned to habitats.

To find the radius of laying, take the size of eggs a cuckoo lays with consider the distance of cuckoos from each other and the present optimum area. Then, the radius (*ELR*) is calculated as Equation (35):

$$ELR = \sigma \times \frac{\text{Size of current cuckoos eggs}}{\text{Total number of eggs}} \times (X_{\max} - X_{\min}) \tag{35}$$

After that, once ELR is calculated, cuckoos will lay their eggs within the nest included in ELR. Once the laying is finished, p% of less profitable eggs (typically 10 %), i.e., the eggs whose suitability function is more petite, will be discarded, and the rest of the newly-born cuckoos will grow up in the nests belonging to the host.

3.1. Migration

Cuckoos continue living in their current area until they grow and seek more suitable places to lay. They do this and move to several regions until the best place is found where all other cuckoos gather to lay eggs. However, as they live in distinctive groups, it is challenging to determine which belongs to which group once they are all together. To resolve this, the K-means method is used to group cuckoos. K usually is 3–5. It is worth noting that the travel path of cuckoos is more than just a direct route. Only λ% of the path is traveled with deflection φ. Cuckoos employ these two parameters to discover more incredible zones, i.e., λ and φ. The first is a random number between [0, 1], while φ is an angle that varies between [−6/π, 6/π]. Overall, the new position (X_i^{new}) by the migration can be formulated as Equation (36):

$$X_i^{new} = X_i + F \times (X_{best} - X_i) \tag{36}$$

Cuckoos travel many times until they find a place (optimal point) where the eggs are more likely to hatch and more food is accessible to the cuckoos. Such a place provides higher profit, and fewer eggs may be destroyed. After the convergence reaches higher than 95 % for all cuckoos and they reach the optimal point, the COA algorithm is terminated.

3.2. Adopting GMM to boost COA

This study propuse a new hybrid algorithm based on COA and GMM as a clustering method to improve the PSO and increase the diversity and adaptability of the algorithm after environment changes.

3.2.1. GMM

A probability density function is a parameter that shows the weighted sum of the density of Gaussian components. This model uses the stabilization of some parameters in each iteration to maximize the probability index. Its related variables are computed using training data and also the iterative Expectation-Maximization (EM) algorithm (mathematical expectation maximization) [87], which is an estimate of the initial model by an ideal training data [87]. The GMM is determined via Equation (37) [88]:

$$p(x|\lambda) = \sum_{i=1}^{M} w_i g\left(x|\mu_i, \sum i\right) \tag{37}$$

where x indicates a d-dimensional continuous data vector (which can be features or sizes), λ representing an initial sample consisting of a set of model parameters $\lambda = \{w_i, \mu_i, \sum i\}$, w_i is the weight of the ith mixture ($\sum_{i=1}^{M} w_i = 1$), M is the size of mixtures and $g(x|\mu_i, \sum i)$ denotes the PDF of Gaussian components. The PDF of any part is a d-dimensional or variable Gaussian function by Equation (38):

$$g\left(x|\mu_i, \sum i\right) = \frac{1}{(2\pi)^{\frac{d}{2}} |\sum i|^{\frac{1}{2}}} exp\left[-\frac{1}{2}(x-\mu_i)^T \left(\sum i\right)^{-1} (x-\mu_i)\right] \tag{38}$$

where μ_i is the mean vector of the ith mixture and $|\sum i|$ is the determinants of the covariance matrix. The complete GMM is parameterized based on all components' mean vectors, density mixture weights, and covariance matrices. GMM parameters are finally introduced in the form of $\lambda = \{w_i, \mu_i, \sum i\}$. There are several techniques for GMM parameter estimation. The Maximum Likelihood (ML) estimation method is the most famous and defined method. ML estimation aims to discover parameters for the model that maximize the probability of GMM according to the training data. Approximations related to ML can be obtained using a special EM algorithm mode. EM uses an iteration cycle to estimate the parameters using a hidden variable λ. The main is to begin a primary model of λ, and compute the novel model $\overline{\lambda}$ in such a way that $p(x|\overline{\lambda}) \geq p(x|\lambda)$. Then it is converted into a primary model for the next generation, and the process has been repeated until it achieves the convergence threshold. The parameters of the model change frequently to maximize the likelihood between the samples and the Gaussian distribution based on these equations [88].

The EM algorithm contains of two parts of calculating mathematical expectation (E) and maximization (M):

- *Part E*

Mathematical expectation, in which GMM parameters are found in any sample of the d-dimensional data $x \in \{x\}_{t=1,\ldots,T}$ using the posterior probability and for the ith component Equation (39) [89]:

$$p(i|x_t, \lambda) = \frac{w_i g(x_t|\mu_i, \sum i)}{\sum_{k=1}^{M} w_i g(x_t|\mu_k, \sum k)} \tag{39}$$

- *Part M*

Maximization, in which the variables are computed via the posterior probability estimated in the previous section, $p(i|x_t,\lambda)$. The posterior probability of the ith Gaussian function is after observing the vector x_t and λ. Parameters of GMM are updated using Equations (40)–(42) [89]:

$$\overline{w_i} = \frac{1}{T}\sum_{i=1}^{T} p(i|x_t,\lambda) \tag{40}$$

$$\overline{\mu_i} = \frac{\sum_{i=1}^{T} p(i|x_t,\lambda)x_t}{\sum_{i=1}^{T} p(i|x_t,\lambda)} \tag{41}$$

$$\overline{\sum i} = \frac{\sum_{i=1}^{T} p(i|x_t,\lambda)\|x_t-\overline{\mu_i}\|^2}{\sum_{i=1}^{T} p(i|x_t,\lambda)} \tag{42}$$

E and M are repeatedly and consequently calculated until the change in parameters of GMM is minimized and the algorithm is converged.

3.2.2. GMMCOA

In the GMMCOA method, we first utilize the GMM algorithm to classify the data into distinct clusters. Each cluster represents a group of similar solutions within the problem space. Subsequently, we apply the COA independently to each cluster. This approach effectively disperses cuckoos throughout the problem space, ensuring adequate exploration and diversity within the population.

- Data Classification with GMM

The GMM algorithm is employed to classify the data into clusters, where each cluster captures a subset of solutions sharing similar characteristics. This clustering process enables the identification of diverse regions within the search space, facilitating more effective exploration by the cuckoos.

- Migration Strategy

Once the data is clustered, the COA algorithm is applied independently to each cluster. This approach ensures that cuckoos are dispersed throughout the problem space, allowing for comprehensive exploration of different regions. The migration strategy employed in GMMCOA involves updating the position of each cuckoo in the search space at each iteration. This update is guided by a combination of factors, including the probability that a cuckoo belongs to a particular cluster and the best global position found by that cluster. By leveraging this probabilistic information, GMMCOA enables cuckoos to navigate the search space more efficiently, leading to faster convergence and improved optimization performance. In GMMCOA, the migration of each cuckoo is updated in the search space at each iteration based on Equation (43):

$$X_i^{new} = X_i^t + rand \times \sum_{k=1}^{K} p\left(C_k|X_i^t\right)\left(X_{best_k}^{\ t} - X_i^t\right) \tag{43}$$

Where K denotes the number of clusters. $X_{best_k}^{\ t}$ represents the best global position found by the kth cluster. $p\left(C_k|X_i^t\right)$ indicates the probability that the ith cuckoo belongs to the kth cluster. *rand* is a random value between 0 and 1.

In this migration strategy, the control parameter F is removed, simplifying the algorithm. Instead, cuckoos utilize probabilistic information from all cuckoos and clusters, enabling faster convergence.

Algorithm 1. represents the pseudocode of the proposed GMMCOA algorithm, outlining the steps involved, including initialization, migration, elimination of less profitable habitats, and updating GMM parameters. By integrating the COA algorithm with GMM clustering, GMMCOA enhances exploration and diversity within the population, leading to improved optimization performance.

Algorithm 1: GMMCOA Algorithm

1. Initialize parameters:
2. - *Npop*: Population size
3. - *D*: Dimensionality of the problem space
4. - *T*: Maximum number of iterations
5. - *p*: Percentage of less profitable eggs to discard
6. - *ELR*: Egg laying radius
7. - λ, φ: Parameters for cuckoo migration
8. - *K*: Number of clusters in GMM
9. Initialize habitat array:
10. - Generate initial population of *Npop* habitats, each with *D* dimensions
11. Initialize GMM:
12. - Cluster data into *K* clusters using GMM algorithm
13. **Main loop**:
14. **for***t* = 1 to *T*:
15. Evaluate fitness of each habitat in the population
16. Migration:
17. **for** each habitat X_i:
18. Cluster habitat X_i into one of *K* clusters
19. Update habitat position:
20. **for** each dimension j = 1 to *D*:
21. Calculate new position X_i^{new} based on equation (43)
22. Eliminate less profitable eggs:
23. Sort habitats based on fitness
24. Discard *p*% of less profitable habitats
25. Update GMM parameters:
26. Perform expectation step (E-step):
27. **for** each data point x_t:
28. Calculate posterior probability $p(i|x_t, \lambda)$ for each cluster
29. Perform maximization step (M-step):
30. Update GMM parameters using equations (40)-(42)
31. Check convergence:
32. **if** convergence criteria met:
33. Terminate algorithm
34. **else**:
35. Continue to next iteration
36. **Endof main loop**

Additionally, the flowchart of the proposed method is shown in Fig. 1. GMMCOA offers several advantages over traditional COA algorithms:

- Enhanced Exploration: The combination of GMM clustering and COA allows for more thorough exploration of the search space.
- Improved Diversity: Clustering ensures that cuckoos are distributed across various regions, promoting population diversity.
- Simplified Algorithm: Removal of the control parameter F simplifies the algorithm, making it easier to implement and tune.

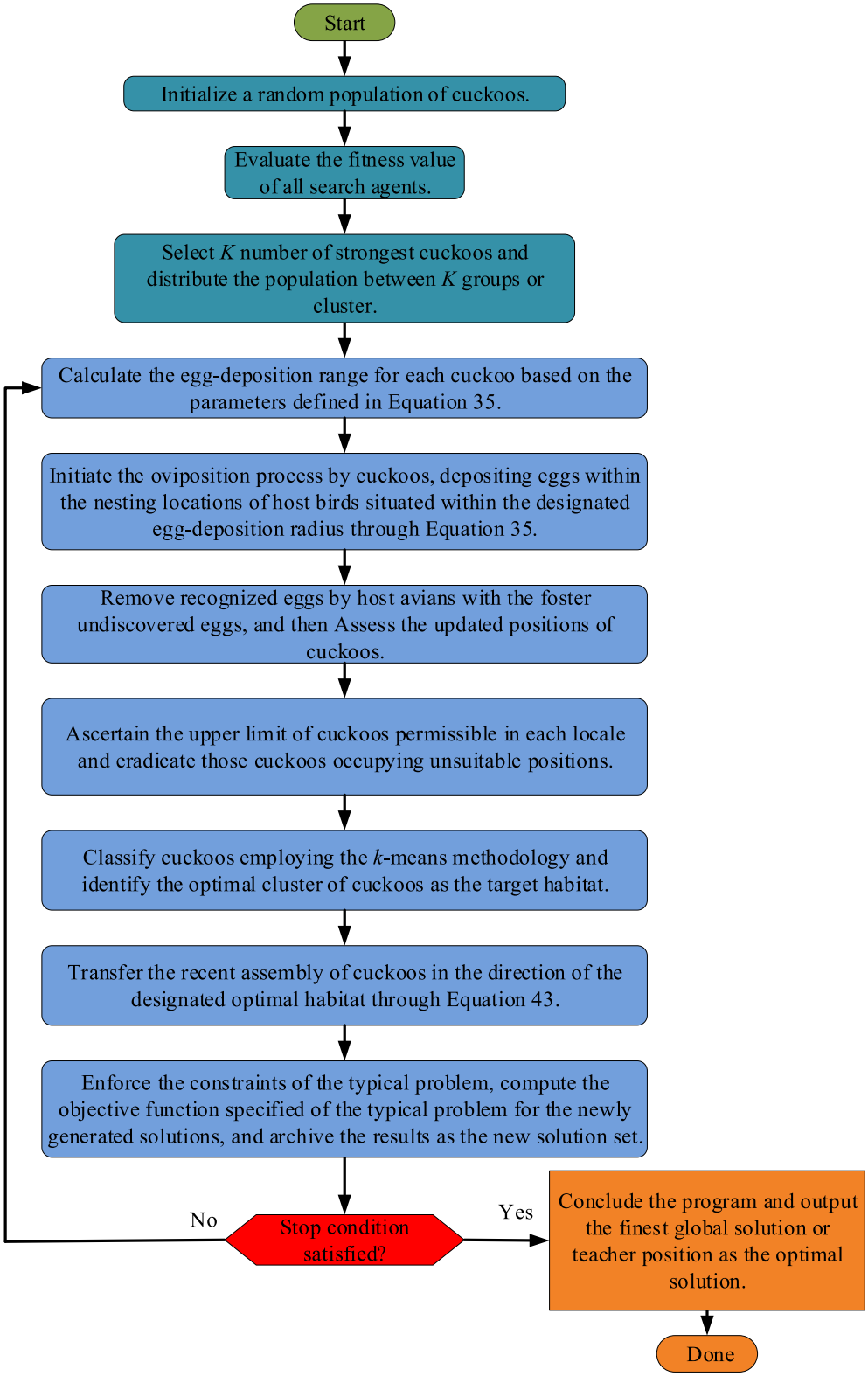

Fig. 1. Flowchart of the GMMCOA algorithm.

- Faster Convergence: Leveraging probabilistic information from all cuckoos and clusters facilitates faster convergence to optimal solutions.

It is noteworthy that recent articles have introduced highly effective methods aimed at enhancing and refining optimization algorithms. These methods have demonstrated significant utility and potency, paving the way for researchers to potentially leverage them in future endeavors to enhance the COA method. Two of these very valuable new proposed methods are methods fitness-distance balance (FDB) [26] and natural survivor method (NSM) [90], which have been successfully used in many algorithms, such as for constrained optimization problems [91], Optimal solution of the combined heat and power economic dispatch [18], and for global optimization and accurate photovoltaic modeling [92].

4. Simulation results

OPF problems are solved in this research by applying the COA and GMMCOA algorithms to the IEEE 30-bus network. The maximum iterations for COA and GMMCOA are 300 for the IEEE 30-bus network, and 1000 IEEE 118-bus network, while the population size is $N_{pop} = 50$ and 40 for the IEEE 30-bus network, and the population size is $N_{pop} = 100$ and 80 for the IEEE 118-bus network, respectively. The data of the system are extracted from Ref. [70]. Simulations are conducted in MATLAB 8.3(R2014*a*) environment using a PC with configuration: 3.0 GHz, 8.0 GB RAM, and core i7 CPU.

The optimization process for solving non-convex OPF problems using the COA and GMMCOA algorithms have been ordered as follows in below:

- Step 1: Establish the initial parameters for GMMCOA based on the parameters inherent to the test system under investigation. Create the initial assembly of population, contingent upon the population size, the lower and upper bounds of control variables, system constraints, and OPF problem limitations, utilizing equations (21)–(30). Stochastically ascertain the present positions of cuckoos to serve as the inaugural solutions for the OPF quandary.
- Step 2: Enforce the constraints of the system and the typical OPF problem, compute the objective function specified in Equation (31) using the matpower package for the initially generated solutions, and archive the results as the initial solution set. Next, Allocate a specific quantity of eggs to each cuckoo.
- Step 3: Calculate the egg-deposition range for each cuckoo based on the parameters defined in Equation (35).
- Step 4: Initiate the oviposition process by cuckoos, depositing eggs within the nesting locations of host birds situated within the designated egg-deposition radius through Equation (35).
- Step 5: Remove recognized eggs by host avians.
- Step 6: Foster undiscovered eggs.
- Step 7: Assess the updated positions of cuckoos.
- Step 8: Ascertain the upper limit of cuckoos permissible in each locale and eradicate those cuckoos occupying unsuitable positions.
- Step 9: Classify cuckoos employing the k-means methodology and identify the optimal cluster of cuckoos as the target habitat.
- Step 10: Transfer the recent assembly of cuckoos in the direction of the designated optimal habitat through Equation (43).
- Step 11: Enforce the constraints of the system and the typical OPF problem, compute the objective function specified in Equation (31) using the matpower package for the newly generated solutions, and archive the results as the new solution set.
- Step 12: Has the algorithm's termination condition been met? If affirmative, conclude the program and output the finest global solution or teacher position as the optimal solution. If negative, proceed to Step 3 and persist with the optimization process.

4.1. OPF of the test system

Locations of generators, transformers, and other system components can be seen in Fig. 2 [50,83]. The apparent base power is 100 MVA, and the demand is 2.834 p.u. limits allowable voltage magnitudes of the load buses have been chosen at 1.05 and 0.95 p.u. The complete dataset for the analyzed system is available in the referenced articles [73,93–96], omitted here to prevent excessive bulkiness in the article.

Table 1 provides OPF results obtained by the proposed method for the system under study without renewables.

4.1.1. Case I: fuel cost minimization

The overall Case I imposed by generating electrical power can be optimized by quadratic Equation (44) [97,98]:

$$J_1 = \sum_{i=1}^{nG} \left(\alpha_i + b_i P_{Gi} + c_i P_{Gi}^2\right) + PF \tag{44}$$

Table 1 reports the results of Case I when the GMMCOA has been used. The obtained best cost is 800.4786 $/h by GMMCOA. As is observed, this algorithm is superior to its counterparts in reducing fuel costs. For instance, some optimization methods, as given in Table 2, include EP [99], SKH [100], ARCBBO [101], AGSO [3], IEP [102], AO [103], FPA [104], ABC [105], TS [106], PPSOGSA [21], MICA-TLA [98], MFO [104], MGBICA [107], PSOGSA [108], GWO [20], DE [20], DE [109], MSA [104], JAYA [47], and MRFO [110]. The results underscore the potency and efficacy of GMMCOA as an innovative optimization algorithm for solving non-convex OPF

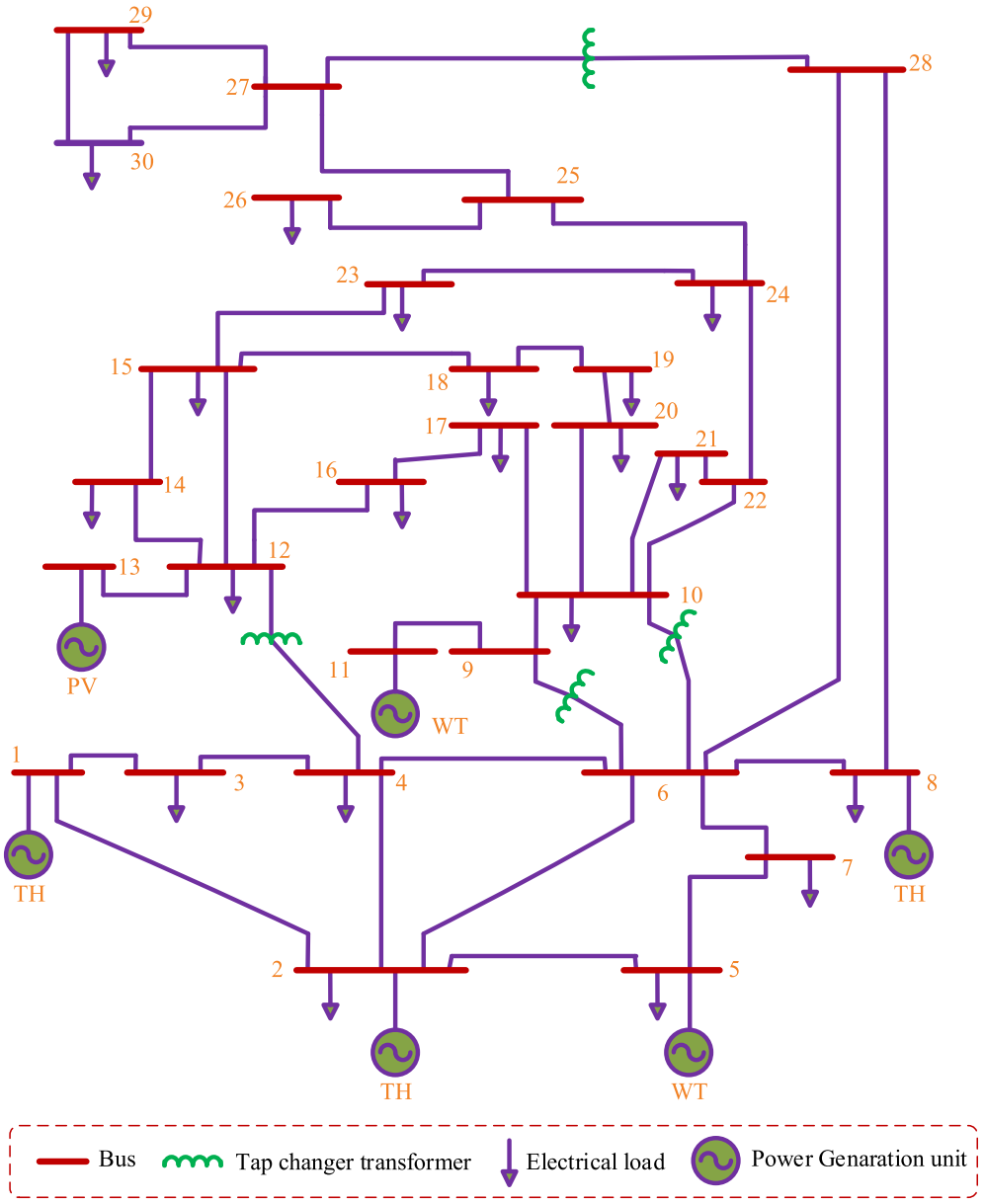

Fig. 2. Single-line diagram of the network.

problems. GMMCOA emerges as a robust competitor in comparison to alternative algorithms. Fig. 3 shows the convergence trend for this case in cost ($/h), that shows that the curve converges in less than 80 iterations.

4.1.2. *Case II: fuel cost with piecewise quadratic objective function*

Equation (45) expresses the mathematical model of the cost due to power generation by fossil fuel-based generating units [97,98]:

$$J_2 = \sum_{k=1}^{n_f} \alpha_{i,k} + b_{i,k} P_{Gi} + c_{i,k} P_{Gi}^2 + PF \tag{45}$$

Table 3 clearly demonstrates that GMMCOA stands out as the most resilient optimization approach for this engineering problem. The outcomes indicate that GMMCOA effectively addressed the optimization challenges posed by the OPF, showcasing its strong optimization capabilities. In fact, the optimal solutions obtained through GMMCOA yielded the lowest fuel cost ($/h)value in the table compared to other optimizers. According to the obtained results in Table 1, the obtained best cost is 646.5364 ($/h) by GMMCOA.

Table 1
Optimal values of the optimization variables found by the GMMCOA method.

Variables optimal values	**Limits**		Cases					
	Lower	Upper	I	II	III	IV	V	VI
P_{G1} (MW)[a]	50	250	177.1475	140.0000	198.7487	102.4767	176.2641	122.2385
P_{G2} (MW)	20	80	48.6972	55.0000	44.8560	55.6679	48.8125	52.5135
P_{G5} (MW)	15	50	21.3903	24.4927	18.4827	38.1382	21.6375	31.4759
P_{G8} (MW)	10	35	21.2556	35.0000	10.0001	35.0000	22.3396	35.0000
P_{G11} (MW)	10	30	11.9301	17.5018	10.0000	30.0000	12.1928	26.7158
P_{G13} (MW)	12	40	12.0000	18.1462	12.0000	26.6462	12.0000	21.0461
V_{G1} (p.u.)	0.95	1.1	1.0837	1.0743	1.0814	1.0684	1.0422	1.0735
V_{G2} (p.u.)	0.95	1.1	1.0606	1.0568	1.0580	1.0565	1.0228	1.0576
V_{G5} (p.u.)	0.95	1.1	1.0340	1.0301	1.0309	1.0344	1.0147	1.0329
V_{G8} (p.u.)	0.95	1.1	1.0383	1.0371	1.0375	1.0424	1.0056	1.0408
V_{G11} (p.u.)	0.95	1.1	1.0985	1.0925	1.0997	1.0730	1.0723	1.0403
V_{G13} (p.u.)	0.95	1.1	1.0517	1.0691	1.0633	1.0677	0.9873	1.0236
$T_{6\text{–}9}$ (p.u.)	0.9	1.1	1.0716	1.0672	1.0346	1.0424	1.0987	1.0999
$T_{6\text{–}10}$ (p.u.)	0.9	1.1	0.9178	0.9005	0.9809	0.9346	0.9000	0.9496
$T_{4\text{-}12}$ (p.u.)	0.9	1.1	0.9769	1.0085	0.9949	1.0049	0.9382	1.0314
$T_{28\text{–}27}$ (p.u.)	0.9	1.1	0.9737	0.9706	0.9782	0.9747	0.9711	1.0047
Q_{C10} (MVAR)	0.0	5.0	2.7569	0.0338	4.7511	4.9879	5.0000	2.8596
Q_{C12} (MVAR)	0.0	5.0	1.1025	0.0033	1.2317	0	0.0239	0.0372
Q_{C15} (MVAR)	0.0	5.0	4.4517	4.9905	4.5143	3.4719	5.0000	3.8463
Q_{C17} (MVAR)	0.0	5.0	5.0000	4.9958	4.9914	5.0000	0.0000	4.9997
Q_{C20} (MVAR)	0.0	5.0	4.2599	4.4971	4.2596	4.2576	5.0000	5.0000
Q_{C21} (MVAR)	0.0	5.0	5.0000	4.9941	4.9942	5.0000	5.0000	5.0000
Q_{C23} (MVAR)	0.0	5.0	3.2688	2.9503	3.2776	3.2591	5.0000	4.2772
Q_{C24} (MVAR)	0.0	5.0	5.0000	4.9968	4.9933	5.0000	5.0000	5.0000
Q_{C29} (MVAR)	0.0	5.0	2.6455	2.6042	2.6249	2.5573	2.6482	2.6157
Cost ($/h)	–	–	800.4786	646.5364	832.1630	859.1852	803.7153	830.2339
VD (p.u.)	–	–	0.9076	0.9174	0.8667	0.9147	0.0946	0.2971
Power losses (MW)	–	–	9.0207	6.7407	10.6875	4.5290	9.8465	5.5898
Emission (t/h)	–	–	0.3663	0.2835	0.4378	0.2288	0.3636	0.2530

[a] P_{G1} is not a control variable; it is the slack generator in the slack bus.

Table 2
Results for case I.

Meta-heuristic	Fuel cost ($/h)	Emission (t/h)	Power losses (MW)	VD (p.u.)	NFEs
EP [99]	803.57	–	–	–	1000
SKH [100]	800.5141	0.3662	9.0282	–	12000
ARCBBO [101]	800.5159	0.3663	9.0255	0.8867	10000
AGSO [3]	801.75	0.3703	–	–	20000
IEP [102]	802.46	–	–	–	16000
AO [103]	801.83	–	–	–	–
FPA [104]	802.7983	0.35959	9.5406	0.36788	5000
ABC [105]	800.660	0.365141	9.0328	0.9209	–
TS [106]	802.29	–	–	–	–
PPSOGSA [21]	800.528	–	9.02665	0.91136	10000
MICA-TLA [98]	801.0488	–	9.1895	–	3000
MFO [104]	800.6863	0.36849	9.1492	0.75768	5000
MGBICA [107]	801.1409	0.3296	–	–	–
PSOGSA [108]	800.49859	–	9.0339	0.12674	10000
GWO [20]	801.41	–	–	–	2700
DE [20]	801.23	–	–	–	2700
HFAJAYA [79]	800.4800	0.3659	9.0134	0.9047	25000
FA [79]	800.7502	0.36532	9.0219	0.9205	25000
DE [109]	802.39	–	9.466	–	2560
MSA [104]	800.5099	0.36645	9.0345	0.90357	5000
JAYA [47]	800.4794	–	9.06481	0.1273	4000
MRFO [110]	800.7680	–	9.1150	–	–
COA	801.7325	0.3752	9.6612	0.5125	15000
GMMCOA	**800.4786**	0.3663	9.0207	0.9076	12000

Table 3 provides some of the methods, including SSO [40], MSA [104], MDE [109], GABC [111], IEP [102], MFO [104], SSA [112], MICA-TLA [98], and FPA [104]. The GMMCOA shows more desirable solutions than these methods. Fig. 4 shows the convergence behavior of the best result by the studied maethods in Case II.

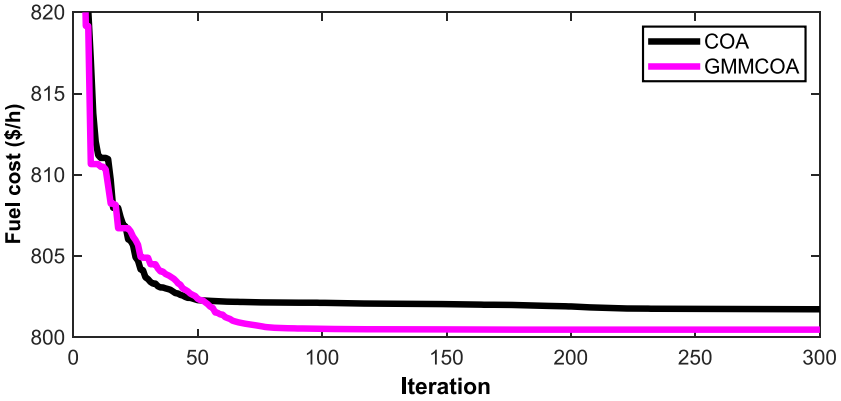

Fig. 3. Convergence behavior in Case I.

Table 3
Results of case II.

Meta-heuristic	Fuel cost ($/h)	Emission (t/h)	Power losses (MW)	VD (p.u.)	NFEs
SSO [40]	663.3518	–	–	–	600
MSA [104]	646.8364	0.28352	6.8001	0.84479	5000
MDE [109]	647.846	–	7.095	–	2560
GABC [111]	647.03	–	6.8160	0.8010	–
IEP [102]	649.312	–	–	–	16000
MFO [104]	649.2727	0.28336	7.2293	0.47024	5000
SSA [112]	646.7796	0.2836	6.5599	0.5320	30000
MICA-TLA [98]	647.1002	–	6.8945	–	3000
FPA [104]	651.3768	0.28083	7.2355	0.31259	5000
COA	648.6003	0.2837	6.8925	0.4863	15000
GMMCOA	**646.5364**	0.2835	6.7407	0.9174	12000

4.1.3. *Case III: considering the valve point effects (VPEs) in the fuel cost*

Equation (46) expresses this objective function when VPEs are considered [97,98]:

$$J_3 = \sum_{i=1}^{n_G} \alpha_i + b_i P_{Gi} + c_i P_{Gi}^2 + \left| e_i \sin\left(f_i\left(P_{Gi}^{\min} - P_{Gi}\right)\right)\right| + PF \tag{46}$$

As per the results in Table 1, the cost when appling GMMCOA has been optimized 832.1630 $/h. We subjected GMMCOA to comparative assessments against widely used optimization techniques in this OPF problem. As depicted in Table 4, the outcomes suggest that the GMMCOA algorithm outperforms the other evaluated algorithms. Hence, it can be deduced that the GMMCOA algorithm possesses the capability to furnish an optimal solution for this OPF problem. Table 4 shows that the latter provides more acceptable results when comparing PSO [54], SP-DE [87], and GMMCOA methods. Fig. 5 illustrates the convergence behavior by COA and GMMCOA in Case III.

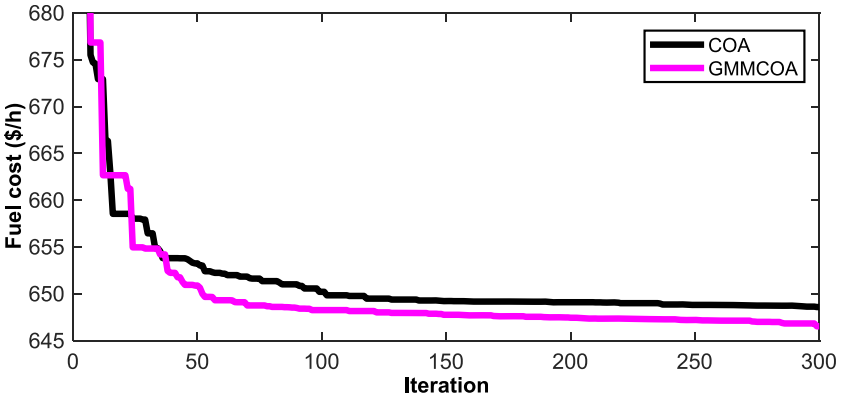

Fig. 4. Convergence behavior in Case II.

Table 4
Results in case III.

Meta-heuristic	Fuel cost ($/h)	Emission (t/h)	Power losses (MW)	VD (p.u.)	NFEs
SP-DE [113]	832.4813	0.43651	10.6762	0.75042	30000
HFAJAYA [79]	832.1798	0.4378	10.6897	0.8578	25000
FA [79]	832.5596	0.4372	10.6823	0.8539	25000
PSO [70]	832.6871	–	–	–	25000
COA	832.9503	0.4388	10.8716	0.7415	15000
GMMCOA	**832.1630**	0.4378	10.6875	0.8667	12000

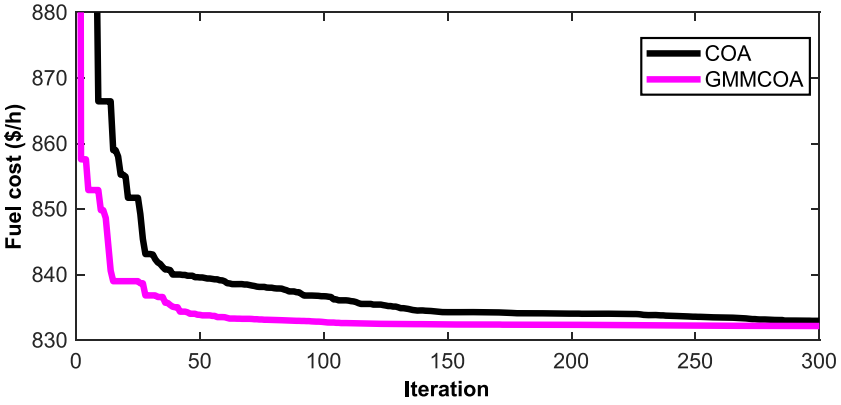

Fig. 5. Convergence behavior in Case III.

Table 5
Results in case IV.

Meta-heuristic	Fuel cost ($/h)	Emission (t/h)	Power losses (MW)	VD (p.u.)	J_4	NFEs
MSA [104]	859.1915	0.2289	4.5404	0.92852	1040.8075	5000
QOMJaya [114]	826.9651	–	5.7596	–	1402.9251	4000
MJaya [114]	827.9124	–	5.7960	–	1059.7524	4000
EMSA [115]	859.9514	0.2278	4.6071	0.7758	1044.2354	–
MOALO [71]	826.4556	0.2642	5.7727	1.2560	1057.3636	–
COA	859.2013	0.2295	4.5702	0.8970	1042.0073	15000
GMMCOA	859.1852	0.2288	4.5290	0.9147	**1040.3452**	12000

The suggested approach was used for cases IV to VI to discover the optimal solutions to multiobjective OPF objective functions under study. Table 1 presents the best solutions among all simulation results when GMMCOA is utilized for these cases.

4.1.4. Fuel cost and power loss

Combining Equations (14) and (19), this objective function can be expressed according to Equation (47).

$$J_4 = \sum_{i=1}^{nG} \left(\alpha_i + b_i P_{Gi} + c_i P_{Gi}^2\right) + \varphi_p P_{Loss} + PF \tag{47}$$

In this formulation, φ_p is set to 40 [104].

As is found, power loss and cost optimized by GMMOCA are respectively 859.1852 $/h and 4.5290 MW. In comparison to MSA [104], QOMJaya [114], MJaya [114], EMSA [115], MOALO [71], and COA, as shown in Table 5, GMMCOA causes to less power loss and fuel cost. The problem showcases the efficacy of the suggested GMMCOA method in addressing a challenge of this specific nature. The optimal solutions for the problem are additionally presented in Table 1 by the suggested GMMCOA method.

Additionally, the convergence trend of this objective function for COA and GMMCOA in Case IV is illustrated in Fig. 6.

4.1.5. Case V: fuel cost and VD

One pillar of ensuring the system is stable and secure is appropriately managing the buses' voltage. This will hopefully result in less voltage deviation. Equation (48) shows a function that simultaneously decreases voltage deviation and fuel cost.

$$J_5 = \sum_{i=1}^{nG} \left(\alpha_i + b_i P_{Gi} + c_i P_{Gi}^2\right) + \varphi_v VD + PF \tag{48}$$

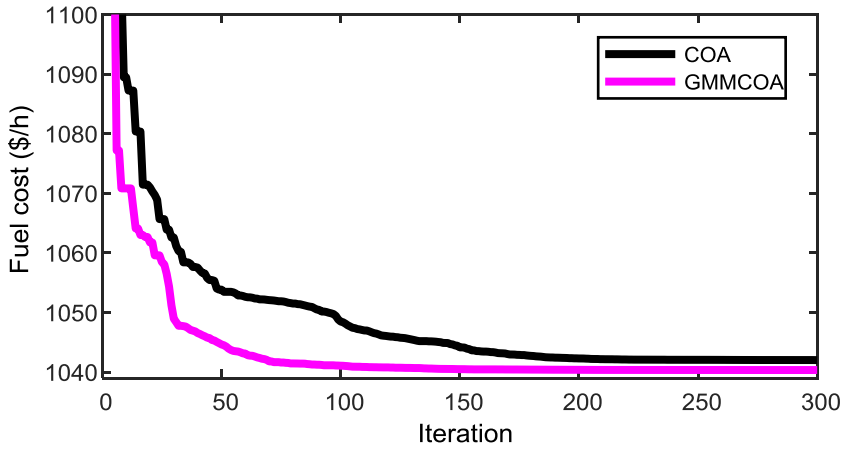

Fig. 6. Convergence behavior in Case IV.

Table 6
Results in case V.

Meta-heuristic	Fuel cost ($/h)	Emission (t/h)	Power losses (MW)	VD (p.u.)	J_5	NFEs
TFWO [9]	803.416	0.365	9.795	0.101	813.5160	20000
MNSGA-II [116]	805.0076	–	–	0.0989	814.8976	24000
MPSO [104]	803.9787	0.3636	9.9242	0.1202	815.9987	5000
MOMICA [116]	804.9611	0.3552	9.8212	0.0952	814.4811	24000
EMSA [115]	803.4286	0.3643	9.7894	0.1073	814.1586	–
BB-MOPSO [116]	804.9639	–	–	0.1021	815.1739	24000
MFO [104]	803.7911	0.36355	9.8685	0.10563	814.3541	5000
COA	804.7040	0.3620	10.1063	0.1010	814.8040	15000
GMMCOA	803.7153	0.3637	9.8484	0.0946	**813.1753**	12000

In (48), φ_v is set to 100 [104].

The voltage deviation with fuel cost, when the GMMCOA is utilized, is found to be 803.7153 $/h and 0.0946 p.u. The optimal solutions for the problem are additionally presented in Table 1 by the suggested GMMCOA method. Table 6 illustrates the results obtained through GMMCOA for the decreases voltage deviation and fuel cost, showcasing its superior performance compared to other algorithms under consideration. In comparison to TFWO [9], MNSGA-II [116], MPSO [104], MOMICA [116], EMSA [115], BB-MOPSO [116], MFO [104], and COA, Table 6 shows that the GMMCOA successfully optimizes the function. Fig. 7 illustrates the convergence trend of the optimal solution achieved by COA and GMMCOA optimizers.

4.1.6. Case VI: VD, emissions, fuel cost, and losses

Equation (49) formulates cases I, V, and IV in one single objective to discover optimal values of voltage deviation, emissions, and fuel cost, with energy losses:

$$J_6 = \sum_{i=1}^{nG} \left(\alpha_i + b_i P_{Gi} + c_i P_{Gi}^2\right) + \varphi_p P_{Loss} + \varphi_v VD + \varphi_e E + PF \tag{49}$$

Weights considered here have been chosen $\varphi_v = 21$, $\varphi_p = 22$, and $\varphi_e = 19$ [104].

Table 7 tabulates the optimal results, in which the GMMCOA provides a more acceptable report for GMMCOA in comparison to MFO [104], J-PPS3 [117], J-PPS1 [117], PSO [118], J-PPS2 [117], MSA [104], MNSGA-II [116], BB-MOPSO [116], SSO [118], MOALO [71], and COA methods. As previously discovered, the GMMCOA is very powerful in discovering the best solution than its counterparts, which are trapped in local minima. Upon scrutinizing the results presented in Table 7, it becomes evident that the outcomes of the majority of scrutinized heuristics closely align with those derived from mathematical optimization and constraint correction. However, a slight variance in findings is observed for one model variable. Furthermore, there is a considerable overlap in the cost function values between the benchmarks in the literature and the evaluated heuristics. Consequently, claiming that the proposed GMMCOA stands out as the superior algorithm among those under consideration would be misleading. Conversely, GMMCOA attains a success rate in experiments comparable to modern algorithms such as MNSGA-II [116] and BB-MOPSO [116]. Consequently, GMMCOA secures the top position in terms of the best results.The optimal solutions for the problem are additionally presented in Table 1 by the suggested GMMCOA method.

Fig. 8 shows the convergence trend of the Case VI when COA and GMMCOA are separately used to solve OPF.

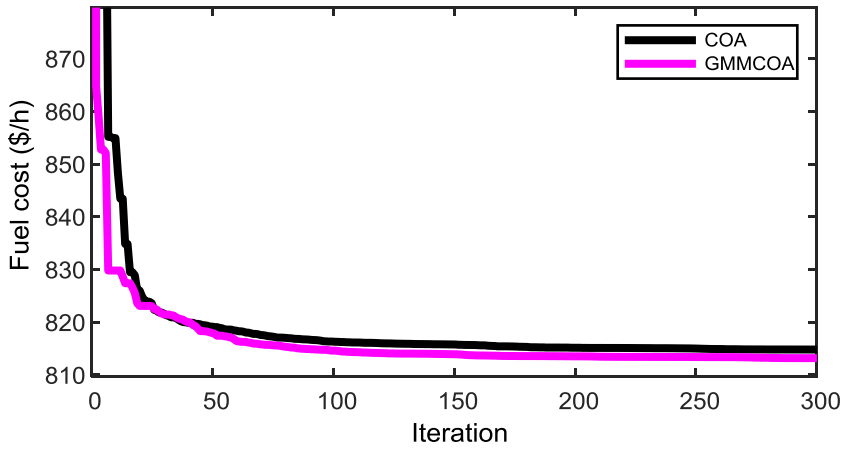

Fig. 7. Convergence behavior in Case V.

Table 7
Results in case IV.

Meta-heuristic	Fuel cost ($/h)	Emission (t/h)	Power losses (MW)	VD (p.u.)	J_6	NFEs
MFO [104]	830.9135	0.25231	5.5971	0.33164	965.8080	5000
J-PPS3 [117]	830.3088	0.2363	5.6377	0.2949	965.0228	6000
J-PPS1 [117]	830.9938	0.2355	5.6120	0.2990	965.2159	6000
J-PPS2 [117]	830.8672	0.2357	5.6175	0.2948	965.1201	6000
MSA [104]	830.639	0.25258	5.6219	0.29385	965.2907	5000
MNSGA-II [116]	834.5616	0.2527	5.6606	0.4308	972.9429	24000
BB-MOPSO [116]	833.0345	0.2479	5.6504	0.3945	970.3379	24000
MOALO [71]	826.2676	0.2730	7.2073	0.7160	1005.0512	–
COA	831.9775	0.2510	5.6879	0.2807	967.7750	15000
GMMCOA	830.2339	0.2530	5.5898	0.2971	**964.2556**	12000

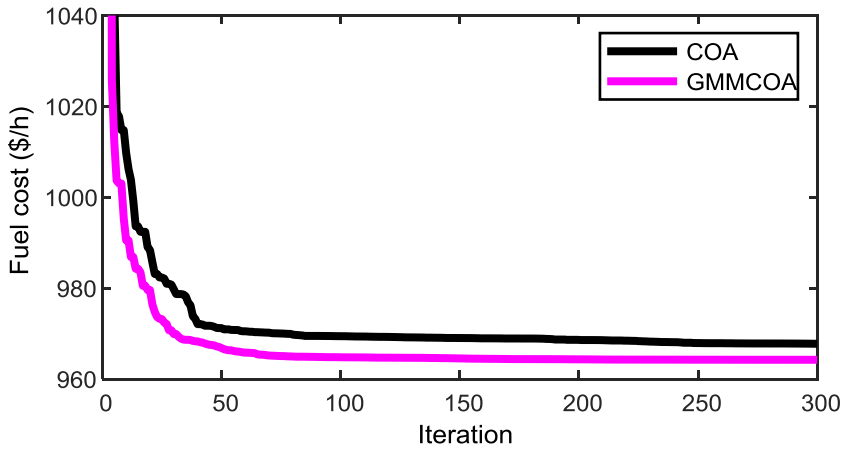

Fig. 8. Convergence behavior in Case IV.

Table 8
Parameters of PDF for WT and PV systems.

Solar PV plant			Wind power plant		
Lognormal mean, Mlgn $G = 483$ W/m2	Lognormal PDF parameters $\mu = 6$, $\sigma = 0.6$	Bus/Rated power (MW) 13/50	$c = 9$, $k = 2$ $c = 10$, $k = 2$ $c = 9$, $k = 2$	$v = 7.976$ m/s $v = 8.862$ m/s $v = 7.976$ m/s	Bus/rated power(MW)/number 5/75/25 11/60/20

Table 9
Optimal parameters in Case VII.

Variables	COA	GMMCOA
$P_{G1} \sim P_{G3}$ (MW)	134.90791, 26.906, 10	134.90791, 27.6625, 10
$Q_{G1} \sim Q_{G3}$ (MVAR)	−2.99051, 1.94584, 40	−1.95876, 13.2061, 35.0016
P_{ws1}, P_{ws2} (MW)	42.7996, 36.2012	43.2743, 36.5399
Q_{ws1}, Q_{ws2} (MVAR)	35, 30	23.2045, 30
P_{ss} (MW)	38.4346	36.7988
Q_{ss} (MVAR)	13.224	17.5628
V_{G1}, V_{G2}, V_{G5}, V_{G8}, V_{G11}, V_{G13} (p.u.)	1.0701, 1.0549, 1.0858, 1.0772, 1.0984, 1.0444	1.0721, 1.0571, 1.035, 1.0397, 1.0998, 1.0552
Solar gen cost ($/h)	106.8895	100.5646
Wind gen cost ($/h)	240.4424	243.2189
Emission (t/h)	1.76248	1.76229
Total Cost ($/h)	782.6373	781.5776
Fuelvlvcost ($/h)	435.3054	437.7941
VD (p.u.)	0.45675	0.46421
Power losses (MW)	5.8493	5.7834

4.2. The 30-bus network with the PV and WT units

4.2.1. Case VII: considering the cost of power generated by PV and WT

This section applies the GMMCOA to the problem of finding the optimum generating cost of energy, WT, and PV systems in the attendance of renewables, such as PV and WT. This is mathematically formulated in Equation (50) [83]:

$$J_7 = \sum_{i=1}^{n_G} \alpha_i + b_i P_{Gi} + c_i P_{Gi}^2 + \left(\sum_{i=1}^{n_w} C_{d,w,i} + C_{ue,w,i} + C_{oe,w,i} \right) + \left(\sum_{i=1}^{n_v} C_{d,pv,i} + C_{ue,pv,i} + C_{oe,pv,i} \right) + \varphi_v VD + PF \tag{50}$$

The fuel coefficients are the equal as in Case I, and the PDF variables are reported in Table 8. The obtained best results from 30 independent runs via COA and GMMCOA optimizers have been listed in Table 9, where P_{ws} is the planned power generation of wind generator WG_1. GMMCOA achieved the best result with more quality and better than COA based on the optimal results. Fig. 9 illustrates the convergence behavior of the cost in Case 7. GMMCOA yields optimal results across all metrics while incurring an equivalent computational cost as COA. The compelling results underscore GMMCOA's competitiveness in addressing this problem. The data unequivocally indicates that GMMCOA contributes to an enhancement in the overall quality of solutions generated by COA.

4.2.2. Case VIII: considering generating cost of energy with the carbon tax

Carbon tax (C_{tax}) is a penalty considered for utilizing fossil fuel-based energy units so that producers are encouraged to adopt

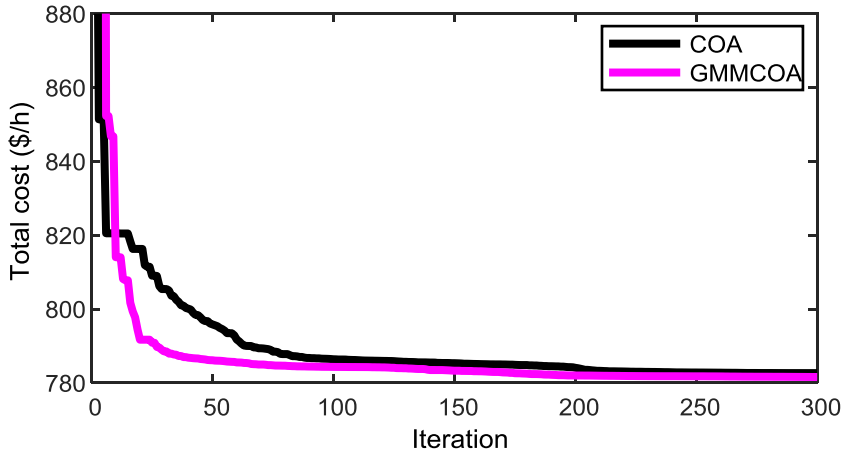

Fig. 9. Convergence behavior in Case VII.

Table 10
Optimal parameters in Case VIII.

Variables	COA	GMMCOA
P_{G1} (MW)	123.76567	123.46248
P_{G2} (MW)	32.1937	32.8806
P_{ws1} (MW)	45.374	45.9368
P_{G3} (MW)	10.0194	10
P_{ws2} (MW)	37.9177	38.6824
P_{ss} (MW)	39.5116	37.725
V_{G1} (p.u.)	1.0695	1.0691
V_{G2} (p.u.)	1.0544	1.0556
V_{G5} (p.u.)	1.0856	1.0345
V_{G8} (p.u.)	1.0362	1.0387
V_{G11} (p.u.)	1.0912	1.1
V_{G13} (p.u.)	1.0857	1.0983
Q_{G1} (MVAR)	−0.14909	−3.531
Q_{G2} (MVAR)	1.4814	10.4774
Q_{ws1} (MVAR)	35	22.4636
Q_{G3}(MVAR)	27.415	31.6386
Q_{ws2} (MVAR)	27.0439	29.7495
Q_{ss} (MVAR)	25	25
Fuelvlvcost ($/h)	427.2243	428.8004
Wind gen cost ($/h)	255.3063	259.9930
Solar gen cost ($/h)	110.9565	104.0033
Total Cost ($/h)	793.4871	792.7967
Emission (t/h)	0.90398	0.88820
J_8	811.5667	810.5607
Carbon tax ($/h)	18.0796	17.764
VD (p.u.)	0.50981	0.53726
Losses (MW)	5.3820	5.2873

cleaner solutions for power production. Emission cost can be formulated by Equation (51) [83]:

$$J_8 = \sum_{i=1}^{n_G} \alpha_i + b_i P_{Gi} + c_i P_{Gi}^2 + \left(\sum_{i=1}^{n_w} C_{d,w,i} + C_{ue,w,i} + C_{oe,w,i} \right) + \left(\sum_{i=1}^{n_v} C_{d,pv,i} + C_{ue,pv,i} + C_{oe,pv,i} \right) + C_{tax} E + PF \tag{51}$$

where, C_{tax} is set at 20 $/ton [83].

Table 10 lists the optimal scheduling of real and reactive generations and overall power generation cost with several other items. Case VIII included the carbon tax, so the influence of PV and WT systems is stronger in Case VIII than in Case VII. The emission level and the rate of applying carbon price are two factors that specify the influence level of renewables. The GMMCOA approach stands out as the most dependable algorithm for achieving precise results, demonstrating its capability to identify the optimal standard deviation in comparison the basic COA.

Furthermore, the COA and GMMCOA convergence trends for Case VIII are illustrated in Fig. 10. The notable convergence speed observed in this scenario serves as compelling evidence of the algorithm's robustness and efficacy.

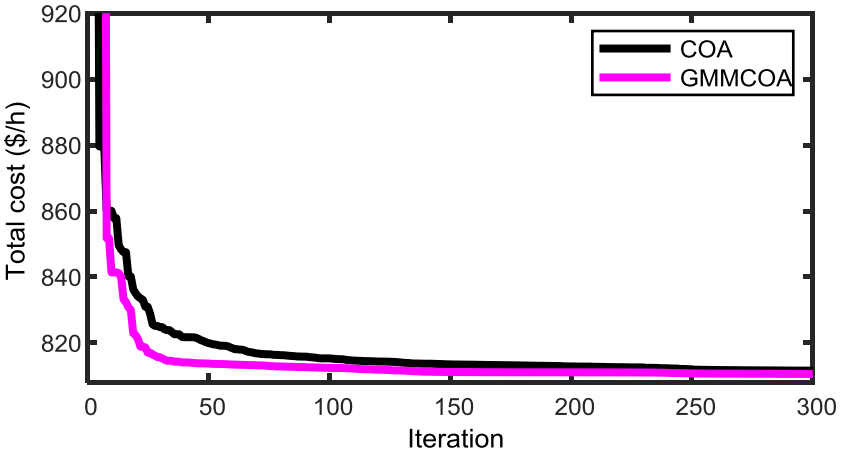

Fig. 10. Convergence behavior in Case VIII.

Table 11
Obtained results related to COA and GMMCOA efficiency.

Meta-heuristic	Best Cost ($/h)	Average Cost ($/h)	Worst Cost ($/h)	standard deviation ($/h)	Time (s)
	Case I				
COA	801.7325	802.3369	802.9659	1.38	17.2
GMMCOA	800.4786	800.6190	800.8224	0.16	14.3
	Case II				
COA	648.6003	648.9921	649.4657	1.04	17.4
GMMCOA	646.5364	646.7287	646.9410	0.40	14.4
	Case III				
COA	832.9503	833.5645	834.7004	1.69	17.3
GMMCOA	832.1630	832.3060	832.5999	0.34	14.4
	Case IV				
COA	1042.0073	1042.5391	1043.3077	1.90	17.2
GMMCOA	1040.3452	1040.5136	1040.7558	0.25	14.2
	CaseV				
COA	814.8040	815.2413	816.0146	2.12	17.3
GMMCOA	813.1753	813.4173	813.6858	0.29	14.4
	Case VI				
COA	967.7750	968.3617	968.9648	0.87	17.3
GMMCOA	964.2556	964.5481	964.8004	0.31	14.3
	Case VII				
COA	782.6373	782.9214	783.6011	0.90	21.2
GMMCOA	781.5776	781.6822	781.9934	0.45	16.9
	Case VIII				
COA	811.5667	812.4104	812.8728	1.24	21.4
GMMCOA	810.5607	810.8038	811.1193	0.37	16.9

Table 12
The effecte if the number of iterations on GMMCOA.

Iterations	Best Cost ($/h)	Average Cost ($/h)	Worst Cost ($/h)	standard deviation ($/h)
	Case I			
100	800.9214	801.0708	801.4127	0.54
300	800.4786	800.6190	800.8224	0.16
400	800.4737	800.6178	800.7995	0.13
800	800.4735	800.6000	800.6847	0.1
	Case VII			
100	781.6237	781.8945	782.5512	0.74
300	781.5776	781.6822	781.9934	0.45
400	781.5768	781.6529	781.8546	0.33
800	781.5721	781.5937	781.7235	0.08

4.3. Statistical comparison

This section presents a comparative study between COA and GMMCOA regarding robustness and sensitivity for all cases. Robustness analysis is often used for investigating complicated issues. To do this, the paper adopts the sensitivity analysis for all case studies.

Table 11 provides the results of this analysis based on the average objective value (i.e., total costs in $/h) of all the solutions (Mean), the best result (Min), the standard deviation (Std.), the average value of the worst results (Max), and the average of time for 30 runs. As observed, the proposed GMMCOA algorithm demonstrates a more robust and reliable performance than the COA. The proposed GMMCOA technique proves to be the most dependable algorithm for achieving precise results, showcasing its ability to determine the optimal standard deviation. The recommended GMMCOA surpasses moderen optimization techniques in terms of solution quality and computational efficiency across the majority of the examined OPF problems. Additionally, the proposed GMMCOA effectively circumvents entrapment in local optima. Consequently, the algorithm introduced in this paper proves to be successful.

4.4. The effect of control parameters on the efficiency of GMMCOA

For this article, after many tests, we have made the best parameters based on our tests and also the reference article. In this part of the article, to learn more about the proposed algorithm, we examine the effect of three parameters, the number of population, the number of repetitions, and the number of clusters on GMMCOA. In the main article, the number of population is 40 and the number of iterations is 300, and the number of clusters is 3. In the first test, we have examined the number of trars with the same conditions as before. It can be seen in Table 12 that by increasing the number of iterations of the algorithm, the swarming of the algorithm is somewhat better and also the best solution is somewhat better. It can be seen in Table 13 that with the increase of the population of the algorithm, the performance of the algorithm will improve to some extent and it will have almost the same performance after the

Table 13
The effecte if the number of population on GMMCOA.

Number of population	Best Cost ($/h)	Average Cost ($/h)	Worst Cost ($/h)	standard deviation ($/h)
	Case I			
20	800.4795	800.9357	801.2416	0.42
40	800.4786	800.6190	800.8224	0.16
60	800.4783	800.6172	800.7071	0.10
80	800.4783	800.6165	800.6630	0.07
	Case VII			
20	781.5782	781.8837	782.6084	0.83
40	781.5776	781.6822	781.9935	0.45
60	781.5770	781.6518	781.8062	0.41
80	781.5764	781.6479	781.7814	0.38

Table 14
The effecte if the number of *K* on GMMCOA.

K	Best Cost ($/h)	Average Cost ($/h)	Worst Cost ($/h)	Standard Deviation ($/h)
	Case I			
2	800.4786	800.9642	801.3720	0.58
3	800.4786	800.6190	800.8224	0.16
5	800.4786	800.6557	800.8529	0.27
	Case VII			
2	781.5780	781.9234	782.2437	0.92
3	781.5776	781.6822	781.9935	0.45
5	781.5776	781.7025	781.1102	0.53

population of 60. In addition, it can be clearly seen from Table 14 that the best number of clusters for the proposed algorithm for OPF problems in this article is equal to 3.

4.5. IEEE 118 bus test network

The effectiveness of the proposed GMMCOA in addressing larger power systems is assessed using the IEEE 118-bus test system [119] in the field of electrical engineering. This test network features 54 generators, 2 reactors, 12 capacitors, 9 transformers, and 186 branches. A total of 129 control variables are considered, encompassing 54 generator active powers and bus voltages, 9 transformer tap settings, and 12 shunt capacitor reactive power injections. Voltage limitations for all buses are maintained between 0.94 and 1.06 p.u. The shunt capacitors offer reactive powers from 0 to 30 MVAR, and transformer tap settings are assessed within the range of 0.90–1.10 p.u [66].

4.5.1. Case 1

The quadratic cost function for conventional generators in OPF, excluding solar and wind energy sources is examined here. In Table 15, the performance of the proposed GMMCOA is juxtaposed with outcomes from alternative algorithms explored in the field of electrical engineering. A comprehensive review of the literature also includes various techniques utilized for solving large-scale OPF problems. The comparative analysis in these tables showcases the superiority of GMMCOA over other optimization methodologies in achieving optimal OPF solutions. The simulation results reveal a noteworthy reduction in cost, with GMMCOA achieving a minimum cost of $129,534.7529 per hour, surpassing the outcomes produced by alternative algorithms.

Table 15
Optimal results for case 1.

Method	Best Cost ($/h)	Average Cost ($/h)	Worst Cost ($/h)	Standard Deviation ($/h)	Time (s)	NFEs
GMMCOA	**129,534.7529**	**129,544.0806**	**129,551.5237**	**8.26**	**618**	80000
COA	130,117.9215	130,208.2103	130,436.4829	74.91	747	100000
Rao-2 [120]	131490.7	–	–	–	804.6	–
GWO [20]	139948.1	142989.3	145484.6	797.8	1766.2	–
FHSA [120]	132,138.3	132,138.3	132,138.3	0.0	–	–
MFO [104]	129708.1	–	–	–	–	5000
FPA [104]	129688.7	–	–	–	–	5000
SSO [120]	132080.4	–	–	–	–	–
MRao-2 [120]	131457.8	–	–	–	1160.3	–
Rao-1 [120]	131817.9	–	–	–	808.0	–
Rao-3 [120]	131793.1	–	–	–	806.7	–
ICBO [70]	135121.6	–	–	–	–	225000
MSA [104]	129640.7	–	–	–	–	5000

Table 16
Optimal results for Case 2.

Method	Best Cost ($/h)	Average Cost ($/h)	Worst Cost ($/h)	Standard Deviation ($/h)	Time (s)	NFEs
GMMCOA	**103382.9225**	**103498.0014**	**103580.6193**	**52.81**	**672**	80000
COA	103400.8230	103546.6255	103617.2849	234.39	795	100000
DEEPSO [66]	103407.6296	103889.1446	104507.4884	292.8782	–	15000
MSA [66]	107695.0619	111205.0554	116303.6361	1857.2167	–	15000
BSA [66]	117149.9833	120443.2982	123385.1256	1638.0949	–	15000
DS [66]	110992.4249	112680.2902	114787.7786	953.6529	–	15000

4.5.2. Case 2

OPF incorporating a quadratic cost function for conventional generators along with the integration of solar and wind energy sources is investigated in this section.

Addressing the OPF challenge involves formulating a quadratic cost function for traditional generators, accounting for their operational costs. Additionally, the inclusion of solar and wind energy sources in this scenario introduces complexities related to their intermittent nature and variable outputs. The overarching goal is to optimize the power flow in the system while considering the unique characteristics and cost implications associated with both traditional and renewable energy sources.

This system is similar to the previous case study, incorporating renewable energy sources at various buses. Wind energy sources are placed at buses 18, 32, 36, 55, 104, and 110, while solar energy generation units are located at buses 6, 15, and 34, respectively.

The optimal solution for this case, obtained through the proposed GMMCOA algorithm, is presented in Table 16 with a comparative study between the results of the algorithms COA and the solutions obtained in Ref. [66]. These results clearly demonstrate that GMMCOA is a highly capable algorithm for optimizing and efficiently distributing loads in large and realistic power systems.

4.5.3. Scalability considerations

The following section focuses on the GMMCOA method's scalability and the challenges associated with applying it to larger and more complex power systems.

- Computational Challenges

Expanding GMMCOA to accommodate larger power systems presents computational obstacles due to increased problem size. As the number of variables and constraints grows, longer computation times and higher memory requirements become apparent. Therefore, optimizing the method's efficiency for larger systems is essential.

- Modeling Complexity

Another challenge is accurately representing the complexities of larger power systems. These systems exhibit more significant variability and uncertainty, requiring advanced techniques to integrate renewable energy effectively, address demand patterns, and incorporate network constraints. Addressing these complexities ensures the resilience and precision of our optimization framework.

- Implementation Considerations

Practical implementation and deployment considerations also impact scalability. Factors such as data availability, communication infrastructure, and system interoperability influence the seamless integration of our method into existing power system management frameworks. Overcoming these challenges requires collaborative efforts and careful planning.

- Mitigation Strategies

Despite these challenges, leveraging parallel and distributed computing techniques offers promising avenues to mitigate scalability issues. By optimizing computational strategies and refining algorithmic approaches, we can enhance the efficiency and scalability of GMMCOA for diverse power system scenarios.

- Commitment to Improvement

In conclusion, while scaling GMMCOA presents challenges, we are dedicated to addressing them through ongoing research and collaboration. By continuously refining our methods and engaging with industry stakeholders, we aim to enhance the scalability and applicability of our approach to meet the evolving needs of larger and more complex power systems.

Table 17
Parameter setting for the test optimization algorithms.

Algorithm	Control parameters
BA	$\gamma = 0.9$, $\alpha = 0.9$ and $r = 0.9$, $Npop = 50$
EHO	$\beta = 0.1$, $\alpha = 0.5$, $clan = 5$
SCA	$a = 2$, $r_1 = a - Iter \times (a/Itermax)$, $r_2 = 2 \times \pi \times$ rand(), $r_3 = 2 \times$ rand(), $r_4 =$ rand()
HHO	E = [-2,2], C = [0, 2], $Npop = 30$
GWO	$Npop = 100$, $a = [2 \rightarrow 0]$
GSA	$\alpha = 20$, $G_0 = 100$, $Npop = 100$
BOA	$c = 0.01$, $\alpha = 0.1$, $p = 0.8$
AWPSO	$c = 0$, $d = 1.5$, $b = 0.5$, $a = 0.000035$, $w = [0.9 \rightarrow 0.4]$

5. Benchmarking and stability analysis with SOTA algorithms

In this section, we conduct a comprehensive assessment of the GMMCOA algorithm alongside various established evolutionary methodologies. To ascertain the distinct efficacy of GMMCOA, we employ the CEC 2017 functions [59] as robust benchmarks for optimization purposes.

The performance evaluation is carried out under consistent conditions with MAX-FEs = 10000D, D = 30, and fmin = 0 across all algorithms. Our comparative analysis includes contemporary approaches drawn from recent research, including GWO [61], BOA [60], AWPSO (a sigmoid-function-based adaptive weighted PSO) [64], GSA [61], BA [62], SCA [60], EHO [60], HHO [63], and COA. Detailed parameter configurations for each algorithm are outlined in Table 17.

The simulation outcomes, presented in Table 18, demonstrate the superior performance of GMMCOA across multiple test functions, underscoring its reliability. Furthermore, upon scrutinizing its effectiveness and robustness on real-world challenges vis-à-vis several enhanced algorithms across all CEC 2017 benchmark functions, GMMCOA consistently delivers satisfactory and commendable results. This firmly establishes GMMCOA as the preferred choice among alternative methodologies.

We also employ the Friedman examination [121–123] to evaluate GMMCOA in comparison to other algorithms across 30 functions. The Friedman assessment rank (*Fr*) nad its mean valve (*MFr*) outcomes are depicted in Table 19. Through Tables 18 and 19, it becomes evident that GMMCOA outperforms its rivals in the majority of functions, with the *MFr* value for GMMCOA standing at 1.2000. This *MFr* value is lower than that of all other methodologies. The optimal solutions derived from this assessment indicate that GMMCOA exhibits significant advantages over all competing approaches.

6. Conclusions

This study introduced and evaluated the integration of GMMCOA, a novel optimization approach that combined Gaussian Mixture Model (GMM) and Cuckoo Optimization Algorithm (COA), for addressing Optimal Power Flow (OPF) challenges in power systems, particularly in the context of Photovoltaic (PV) and Wind Turbine (WT) systems. The extensive evaluation of GMMCOA revealed its robust performance, showcasing rapid convergence and adept handling of local optima across various scenarios.

The statistical analysis based on eight test cases provided valuable insights into the efficacy of GMMCOA in non-convex OPF scenarios. The method consistently outperformed other approaches, demonstrating superior solutions in baseline and sub-case scenarios. The integration of PV and WT systems within the GMMCOA algorithm further enhanced its applicability, ensuring satisfactory outcomes. Comparative analyses against established counterparts underscored the effectiveness of GMMCOA, exhibiting notable advantages in terms of solution quality and computational efficiency. The algorithm excelled in minimizing total cost while effectively managing critical system constraints. In conclusion, GMMCOA emerged as a robust and innovative solution for stochastic OPF problems, with demonstrated efficiency in practical scenarios involving electrical networks. The study suggested promising avenues for future research, including the exploration of multiobjective optimization versions incorporating considerations for renewable energy. The findings positioned GMMCOA as a valuable contribution to the field of power system optimization, offering a reliable and efficient approach to address complex challenges.

Future research directions include extending the algorithm to multiobjective optimization, integrating more renewable sources, addressing real-world implementation challenges, exploring cybersecurity aspects, and evaluating responses to policy changes. Validation on larger grids and consideration of energy storage systems will enhance practical applicability. These avenues ensure ongoing contributions to optimization methodologies in evolving power system landscapes.

Table 18
Evaluation of the evolutionary methods for CEC 2017.

Function	GWO	BOA	AWPSO	GSA	BA	SCA	HHO	EHO	COA	GMMCOA
	Mean	Mean	Mean	Mean	Mean	Mean	Mean	Mean	Mean	Mean
	Std.	Std.	Std.	Std.	Std.	Std.	Std.	Std.	Std.	Std.
	Winner	Winner	Winner	Winner	Winner	Winner	Winner	Winner	Winner	
f_1	1.72E+03	4.47E+10	2.46E+09	1.90E+03	3.37E+11	1.25E+10	1.04E+07	2.68E+10	2.61E-01	1.42E-14
	8.91E+08	6.73E+09	2.67E+09	1.03E+03	3.48E+09	2.94E+09	1.87E+06	5.87E+09	5.96E-01	0.00E+00
	–	–	–	–	–	–	–	–	–	
f_3	2.82E+04	6.48E+04	1.00E+04	8.27E+04	2.85E+09	3.47E+04	4.85E+03	7.23E+04	2.62E+03	1.14E-08
	9.70E+03	9.30E+03	2.12E+04	4.33E+03	4.62E+08	7.52E+03	1.70E+03	9.76E+03	1.14E+03	1.28E-08
	–	–	–	–	–	–	–	–	–	
f_4	1.70E+02	1.94E+04	2.81E+02	1.42E+02	3.54E+04	1.05E+03	1.25E+02	4.60E+03	3.90E+02	9.95E+01
	4.98E+01	3.77E+03	1.76E+02	1.59E+01	1.36E+03	3.75E+02	2.36E+01	3.91E+02	3.02E+02	9.23E+01
	–	–	–	–	–	–	–	–	–	
f_5	9.20E+01	3.71E+02	8.15E+01	2.26E+02	5.26E+03	2.73E+02	2.30E+02	3.34E+02	2.59E+02	1.05E+02
	2.63E+01	2.33E+01	2.75E+01	2.01E+01	2.13E+01	2.24E+01	2.98E+01	1.80E+01	9.61E+02	1.06E+01
	+	–	+	–	–	–	–	–	–	
f_6	4.00E+00	7.00E+01	4.12E+00	5.00E+01	6.85E+02	4.90E+01	6.34E+01	7.10E+01	6.48E-01	5.29E-06
	2.33E+00	9.54E+00	3.05E+00	2.75E+00	6.55E+00	5.20E+00	5.40E+00	6.00E+00	9.93E-01	9.07E-06
	–	–	–	–	–	–	–	–	–	
f_7	1.35E+02	6.10E+02	1.12E+02	8.70E+01	1.80E+03	4.40E+02	5.30E+02	7.30E+02	5.84E+01	3.51E+01
	4.95E+01	5.58E+01	2.23E+01	1.19E+01	1.63E+02	4.15E+01	8.35E+01	4.43E+01	1.13E+01	4.50E+01
	–	–	–	–	–	–	–	–	–	
f_8	8.10E+01	3.00E+02	8.02E+01	1.51E+02	1.65E+04	2.50E+02	1.69E+02	3.00E+02	5.72E+01	1.11E+01
	1.25E+01	1.85E+01	2.33E+01	1.31E+01	3.98E+01	1.62E+01	2.33E+01	2.15E+01	7.61E+00	8.89E+00
	–	–	–	–	–	–	–	–	–	
f_9	2.80E+02	8.45E+03	3.52E+02	2.03E+03	1.01E+04	4.81E+03	5.86E+03	8.48E+03	8.48E+00	1.51E-01
	1.39E+02	1.03E+03	4.08E+02	3.92E+02	1.69E+03	1.43E+03	5.95E+02	1.20E+03	1.14E+00	2.35E-01
	–	–	–	–	–	–	–	–	–	
f_{10}	2.73E+03	7.49E+03	2.85E+03	3.87E+03	9.88E+04	7.04E+03	4.39E+03	7.15E+03	4.04E+03	1.19E+03
	5.49E+02	2.75E+02	6.26E+02	4.34E+02	7.65E+03	3.42E+02	6.57E+02	3.14E+02	2.13E+03	1.08E+02
	–	–	–	–	–	–	–	–	–	
f_{11}	4.10E+02	4.51E+03	2.00E+02	3.50E+02	3.46E+04	1.05E+03	1.52E+02	1.03E+03	1.16E+02	3.69E+01
	4.42E+02	1.83E+03	1.11E+02	8.92E+01	3.37E+03	2.65E+02	3.99E+01	1.46E+02	4.99E+02	2.86E+01
	–	–	–	–	–	–	–	–	–	
f_{12}	3.31E+07	1.05E+10	1.61E+08	1.03E+07	3.95E+09	1.13E+09	9.24E+06	3.17E+09	1.08E+05	1.20E+04
	3.81E+07	3.41E+09	3.26E+08	1.93E+07	9.45E+07	2.52E+08	5.95E+06	5.20E+08	5.39E+05	1.06E+04
	–	–	–	–	–	–	–	–	–	
f_{13}	6.63E+06	6.52E+09	3.91E+07	2.97E+04	4.17E+09	3.87E+08	3.14E+05	1.06E+09	1.94E+03	8.90E+01
	2.33E+07	3.65E+09	1.93E+08	6.45E+03	6.17E+08	1.24E+08	1.17E+05	2.71E+08	7.23E+03	3.09E+01
	–	–	–	–	–	–	–	–	–	
f_{14}	7.96E+04	9.60E+05	1.79E+04	4.73E+05	1.35E+07	1.42E+05	5.19E+04	1.79E+05	3.02E+01	4.78E+01
	1.76E+05	1.84E+06	3.34E+04	1.31E+05	1.65E+06	8.76E+04	1.03E+05	7.54E+04	2.59E+00	4.56E+00
	–	–	–	–	–	–	–	–	+	
f_{15}	2.43E+05	1.35E+08	4.20E+04	1.02E+04	1.73E+08	1.19E+07	6.89E+04	2.60E+07	1.85E+02	2.90E+01
	5.82E+05	1.80E+08	6.34E+04	1.93E+03	6.11E+07	1.07E+07	6.59E+04	1.04E+07	7.91E+02	4.09E+00
	–	–	–	–	–	–	–	–	–	
f_{16}	7.20E+02	4.58E+03	8.18E+02	1.58E+03	4.46E+04	2.01E+03	1.60E+03	2.57E+03	2.49E+03	4.67E+02
	2.39E+02	1.38E+03	2.88E+02	2.84E+02	2.96E+02	3.47E+02	3.65E+02	1.94E+02	2.03E+03	2.40E+02
	–	–	–	–	–	–	–	–	–	

(*continued on next page*)

Table 18 (*continued*)

Function	GWO	BOA	AWPSO	GSA	BA	SCA	HHO	EHO	COA	GMMCOA
	Mean	Mean	Mean	Mean	Mean	Mean	Mean	Mean	Mean	Mean
	Std.	Std.	Std.	Std.	Std.	Std.	Std.	Std.	Std.	Std.
	Winner	Winner	Winner	Winner	Winner	Winner	Winner	Winner	Winner	
f_{17}	2.30E+02	6.17E+03	3.11E+02	1.20E+03	3.07E+04	7.10E+02	9.54E+02	8.90E+02	7.51E+02	8.61E+01
	1.16E+02	5.38E+03	1.58E+02	1.70E+02	1.82E+02	1.88E+02	2.84E+02	1.65E+02	7.01E+02	2.92E+01
	–	–	–	–	–	–	–	–	–	
f_{18}	7.73E+05	1.08E+07	5.66E+05	3.18E+05	2.26E+09	3.92E+06	8.29E+05	1.38E+06	2.02E+03	6.09E+01
	1.40E+06	1.50E+07	1.02E+06	1.76E+05	1.98E+07	2.66E+06	7.16E+05	6.64E+05	7.74E+02	2.34E+01
	–	–	–	–	–	–	–	–	–	
f_{19}	2.04E+05	2.64E+08	2.47E+05	1.23E+04	1.66E+09	2.13E+07	2.41E+05	6.23E+07	1.15E+03	2.19E+01
	3.88E+05	2.69E+08	7.76E+05	5.13E+03	6.24E+07	1.10E+07	1.77E+05	2.53E+07	3.89E+03	1.46E+00
	–	–	–	–	–	–	–	–	–	
f_{20}	3.30E+02	8.40E+02	2.99E+02	1.03E+03	3.96E+03	6.30E+02	7.37E+02	5.80E+02	1.47E+02	2.99E+01
	1.66E+02	1.04E+02	1.27E+02	2.36E+02	1.36E+02	1.01E+02	2.12E+02	7.75E+01	1.69E+02	2.19E+01
	–	–	–	–	–	–	–	–	–	
f_{21}	2.70E+02	3.90E+02	2.94E+02	4.60E+02	2.87E+03	4.50E+02	4.60E+02	5.00E+02	3.27E+02	2.95E+02
	1.85E+01	1.51E+02	1.75E+01	1.95E+01	2.55E+01	1.50E+01	5.25E+01	1.60E+01	8.45E+01	3.08E+01
	+	–	–	–	–	–	–	–	–	
f_{22}	2.27E+03	2.20E+03	2.12E+03	4.19E+03	5.33E+04	5.98E+03	4.23E+03	2.99E+03	5.81E+03	2.08E+03
	1.45E+03	7.00E+02	1.46E+03	1.69E+03	1.70E+03	2.36E+03	1.77E+03	3.14E+02	1.18E+04	3.08E+03
	–	–	–	–	–	–	–	–	–	
f_{23}	4.30E+02	9.00E+02	5.90E+02	1.26E+03	3.37E+04	6.80E+02	8.07E+02	9.90E+02	6.75E+02	4.48E+02
	3.04E+01	1.23E+02	7.49E+01	1.23E+02	4.95E+02	2.64E+01	1.05E+02	5.15E+01	5.21E+01	1.13E+01
	+	–	–	–	–	–	–	–	–	
f_{24}	5.00E+02	1.37E+03	7.13E+02	8.90E+02	5.77E+04	7.60E+02	1.05E+03	1.08E+03	4.56E+02	3.39E+02
	4.70E+01	1.67E+02	1.18E+02	5.57E+01	5.19E+05	2.46E+01	1.47E+02	6.37E+01	1.12E+01	1.27E+01
	–	–	–	–	–	–	–	–	–	
f_{25}	4.60E+02	3.15E+03	4.11E+02	4.30E+02	4.95E+05	6.70E+02	4.10E+02	2.22E+03	3.87E+02	3.87E+02
	2.69E+01	4.64E+02	7.28E+01	1.22E+01	4.86E+07	7.39E+01	2.02E+01	5.33E+02	2.76E-01	2.43E-01
	–	–	–	–	–	–	–	–	=	
f_{26}	1.83E+03	7.80E+03	2.29E+03	4.26E+03	7.85E+04	4.33E+03	3.75E+03	6.00E+03	2.43E+03	1.50E+03
	2.45E+02	1.17E+03	7.62E+02	8.95E+02	6.76E+02	3.06E+02	2.12E+03	5.87E+02	2.07E+02	1.39E+02
	–	–	–	–	–	–	–	–	–	
f_{27}	5.30E+02	1.06E+03	6.09E+02	1.97E+03	3.65E+04	6.90E+02	6.31E+02	1.23E+03	5.11E+02	5.05E+02
	1.78E+01	1.35E+02	9.38E+01	3.21E+02	6.75E+01	2.60E+01	6.78E+01	9.38E+01	8.51E+00	3.97E+00
	–	–	–	–	–	–	–	–	–	
f_{28}	5.30E+02	5.05E+03	6.06E+02	5.10E+02	5.64E+04	1.03E+03	4.52E+02	2.29E+03	4.53E+02	3.70E+02
	4.83E+01	5.08E+02	1.60E+02	4.94E+01	4.33E+02	1.63E+02	2.65E+01	3.00E+02	5.87E+01	7.79E+01
	–	–	–	–	–	–	–	–	–	
f_{29}	8.10E+02	6.47E+03	5.19E+02	1.81E+03	5.46E+04	1.69E+03	1.37E+03	2.30E+03	6.78E+02	5.74E+02
	1.26E+02	2.74E+03	1.70E+02	2.10E+02	3.57E+02	2.52E+02	2.96E+02	2.14E+02	1.06E+02	9.66E+01
	–	–	+	–	–	–	–	–	–	
f_{30}	3.90E+06	5.74E+08	5.15E+05	1.67E+05	1.65E+09	7.06E+07	1.65E+06	8.97E+07	2.62E+04	2.04E+03
	3.10E+06	3.63E+08	9.02E+05	1.24E+05	6.31E+07	3.47E+07	8.27E+05	3.04E+07	1.21E+04	9.60E+01
	–	–	–	–	–	–	–	–	–	
+/−/ =	**3/26/0**	**0/29/0**	**2/27/0**	**0/29/0**	**0/29/0**	**0/29/0**	**1/28/0**	**1/28/0**	**1/27/1**	–

Table 19
Evaluation of the evolutionary methods for CEC 2017.

Function	GWO	BOA	AWPSO	GSA	BA	SCA	HHO	EHO	COA	GMMCOA
	Fr	Fr	Fr	Fr	Fr	Fr	Fr	Fr	Fr	Fr
f_1	2	9	6	4	10	7	5	8	2	1
f_3	5	7	4	9	10	6	3	8	2	1
f_4	4	9	5	3	10	7	2	8	6	1
f_5	2	9	1	4	10	7	5	8	6	3
f_6	3	9	4	6	8	5	7	10	2	1
f_7	5	8	4	3	10	6	7	9	2	1
f_8	4	8.5	3	5	10	7	6	8.5	2	1
f_9	3	8.5	4	5	10	6	7	8.5	2	1
f_{10}	2	9	3	4	10	7	6	8	5	1
f_{11}	6	9	4	5	10	7.5	3	7.5	2	1
f_{12}	5	10	6	4	9	7	3	8	2	1
f_{13}	5	10	6	3	9	7	4	8	2	1
f_{14}	5	9	3	8	10	6	4	7	1	2
f_{15}	6	10	4	3	9	7	5	8	2	1
f_{16}	2	10	3	4.5	9	6	4.5	8	7	1
f_{17}	2	9	3	8	10	4	7	6	5	1
f_{18}	5	9	4	3	10	8	6	7	2	1
f_{19}	4	9	5.5	3	10	7	5.5	8	2	1
f_{20}	4	8	3	9	10	6	7	5	2	1
f_{21}	1	5	3	7.5	10	6	7.5	9	4	2
f_{22}	3.5	3.5	1.5	6.5	10	9	6.5	5	8	1.5
f_{23}	1	7	3	9	10	4.5	6	8	4.5	2
f_{24}	2.5	9	4	6	10	5	7.5	7.5	2.5	1
f_{25}	6	9	3.5	5	10	7	3.5	8	1.5	1.5
f_{26}	2	9	3	6	10	7	5	8	4	1
f_{27}	3	7	4	9	10	6	5	9	2	1
f_{28}	5	9	6	4	10	7	2.5	8	2.5	1
f_{29}	4	9	1	6	10	7	5	8	3	2
f_{30}	6	9	4	3	10	7	5	8	2	1
MFr	3.6000	8.2167	3.6167	5.1833	9.4667	6.3000	5.0167	7.5667	3.0000	**1.2000**
Totlal rank	3	9	4	6	10	7	5	8	2	**1**

Data availability statement

Data sharing is not applicable to this article as no new data were created or analyzed in this study.

Nomenclature

i	Index representing the power unit or generator.
j	Index representing the network line.
n_G	Number of power units or generators.
n_f	Number of fuel alternatives for a generator.
N_l	Number of network lines.
n_{PQ}	Number of buses with a load.
P_{Gi}	Generation of the i th power unit (MW).
V_i	Voltage of bus i.
δ_{ij}	Voltage phase angle difference between buses i and j.
VLi	Voltage magnitude of bus i (p.u.).
J	Fuel cost function ($/h).
$f_i(P_{Gi})$	Cost function of the i th power unit ($/h).
E	Cost function of pollutant gases (ton/h).
P_{Loss}	Cost function related to power losses on the lines (MW).
VD	Cost function of voltage deviation (p.u.).
α_i, β_i, γ_i, ξ_i, θ_i	Coefficients related to the emission of pollutant gases for the i th power unit.
$\alpha_{i,k}$, $\beta_{i,k}$, $\gamma_{i,k}$	Coefficients of the generator for the k th fuel alternative.
a_i, b_i, c_i	Coefficients of the cost related to the i th power unit.
e_i, f_i	Cost coefficients related to the valve point for generator i.
α_i, β_i, γ_i, ξ_i	Coefficients related to the emission of pollutant gases for the i th power unit.
α_i, b_i, c_i	Coefficients of the fuel cost function for the i th power unit.
G_{ij}, B_{ij}	Imaginary and real sections of the element on row i and column j of the admittance matrix.
$P_{Gi} - P_{Di}$	Real power generation minus real power demand at bus i (MW).
$Q_{Gi} - Q_{Di}$	Reactive power generation minus reactive power demand at bus i (MVAR).
V_i	Voltage magnitude at bus i (p.u.).
δ_{ij}	Voltage phase angle difference between buses i and j.
n	Number of buses.

(*continued on next page*)

(*continued*)

$V_i^{\min}$, $V_i^{\max}$	Minimum and maximum boundaries of voltage magnitude at bus i (p.u.).
n_G	Number of generating units.
$P_{Gi}^{\min}$, $P_{Gi}^{\max}$	Minimum and maximum limits on active power produced by unit i (MW).
$Q_{Gi}^{\min}$, $Q_{Gi}^{\max}$	Minimum and maximum limits on reactive power produced by unit i (MVAR).
$T_i^{\min}$, $T_i^{\max}$	Minimum and maximum limits on tap-changer of transformer i.
N_{tab}	Number of tap-changers.
$Q_{c,i}^{\min}$, $Q_{c,i}^{\max}$	Minimum and maximum limits on shunt compensator i (MVAR).
N_{cap}	Number of capacitors.
$S_i^{\max}$	Maximum MVA capacity of transmission line i.
N_l	Number of transmission lines.
$P_{w,i}$, $P_{w,r,i}$	Generation power and rated generation power of wind turbine i (MW).
$P_{pv,i}$, $P_{pv,r,i}$	Generation power and rated generation power of PV unit i (MW).
J	Fundamental objective function incorporating penalty terms to check constraint violations.
$f_i(P_{Gi})$	Cost function of the i th power unit ($/h).
PF	Penalty factor to check constraint violations.
λ_P, λ_Q, λ_V, λ_S	Penalty coefficients.
P_{G1}, Q_{Gi}, VLi, S_{li}	Generation power of the first generator, reactive power of generator i, voltage magnitude of bus i, and MVA capacity of transmission line i, respectively.
$P_{G1}^{\lim}$, $Q_{Gi}^{\lim}$, $VLi^{\lim}$, $S_{li}^{\lim}$	Limits on generation power, reactive power, voltage magnitude, and MVA capacity, respectively.
n_G	Number of power units.
NPQ	Number of buses with loads.
N_l	Number of transmission lines.
n_w	Number of wind sources.
n_v	Number of PV sources.
$P_{w,i}$	Scheduled wind power output of the i th wind turbine (MW).
$P_{pv,i}$	Scheduled power output of the i th PV source (MW).
$d_{w,i}$	Direct cost coefficient related to the i th wind turbine ($/MWh).
$d_{pv,i}$	Direct cost coefficient related to the i th PV source ($/MWh).
P_i	Energy generation by wind turbines or PV sources (MW).
$P_{w,r,i}$	Rated output power of the i th wind turbine (MW).
$P_{pv,r,i}$	Rated output power of the i th PV source (MW).
$V_{w,r}$	Rated speed of the wind (m/s).
$V_{w,in}$	Cut-in speed of the wind (m/s).
$V_{w,out}$	Cut-out speed of the wind (m/s).
C	Scale variable related to the Weibull Probability Density Function (PDF) of wind speed.
K	Shape variable related to the Weibull PDF of wind speed.
α, β	Parameters of the beta distribution representing the PDF of irradiance.
R	Irradiation (W/ m^2).
$C_{d,w,i}$	Cost function for the output power of the i th wind turbine ($/h).
$C_{oe,w,i}$	Cost of overestimation for the i th wind turbine ($/h).
$C_{ue,w,i}$	Cost of underestimation for the i th wind turbine ($/h).
$K_{oe,w,i}$	Reserve cost factor of the i th wind turbine.
$K_{ue,w,i}$	Penalty cost factor of the i th wind turbine.
$C_{d,pv,i}$	Cost function for the output power of the i th PV source ($/h).
$C_{oe,pv,i}$	Cost of overestimation for the i th PV source ($/h).
$C_{ue,pv,i}$	Cost of underestimation for the i th PV source ($/h).
$K_{oe,pv,i}$	Reserve cost factor of the i th PV source.
$K_{ue,pv,i}$	Penalty cost factor of the i th PV source.
COS $T_{w,i}$	Overall cost associated with the i th wind turbine ($/h).
COS $T_{pv,i}$	Overall cost associated with the i th PV source ($/h).
$f(P_i)$	PDF of energy generation by wind turbines or PV sources.
$f(R)$	PDF of irradiance.
R_C, R_{STD}	Irradiance levels (W/ m^2).
X_i	Current position vector of cuckoo i.
$f(X_i)$	Profit (suitability) function of a habitat or cuckoo i.
N_{pop}	Number of cuckoos in the population.
D	Dimensionality of the search space.
ELR	Radius of laying eggs.
σ	Scaling factor.
$X_{\max}, X_{\min}$	Maximum and minimum bounds of the search space.
λ, φ	Parameters controlling cuckoo migration.
X_{best}	Best global position found by a cluster.
K	Number of clusters.
$p(C_k \mid X_i^t)$	Probability that cuckoo i belongs to cluster k.

CRediT authorship contribution statement

Ali S. Alghamdi: Writing – original draft, Validation, Software, Resources, Project administration, Methodology, Investigation, Formal analysis, Data curation, Conceptualization. **Mohamed A. Zohdy:** Supervision.

Declaration of competing interest

The authors declare that they have no known competing financial interests or personal relationships that could have appeared to influence the work reported in this paper.

Acknowledgments

The author extends the appreciation to the Deanship of Postgraduate Studies and Scientific Research at Majmaah University for funding this research work through the Project Number (R-2024-1129).

References

[1] T.T. Nguyen, T.T. Nguyen, M.Q. Duong, An improved equilibrium optimizer for optimal placement of photovoltaic systems in radial distribution power networks, Neural Comput. Appl. (2022) 1–30.
[2] T.T. Nguyen, T.T. Nguyen, A.V. Truong, Q.T. Nguyen, T.A. Phung, Multi-objective electric distribution network reconfiguration solution using runner-root algorithm, Appl. Soft Comput. 52 (2017) 93–108.
[3] J. Hazra, A.K. Sinha, A multi-objective optimal power flow using particle swarm optimization, Eur. Trans. Electr. Power 21 (2011) 1028–1045, https://doi.org/10.1002/etep.494.
[4] A. Maheshwari, Y.R. Sood, Solution approach for optimal power flow considering wind turbine and environmental emissions, Wind Eng. 46 (2022) 480–502.
[5] T.T. Nguyen, T.T. Nguyen, An improved cuckoo search algorithm for the problem of electric distribution network reconfiguration, Appl. Soft Comput. 84 (2019) 105720.
[6] V. Tiwari, H.M. Dubey, M. Pandit, Assessment of optimal size and location of DG/CB in distribution systems using coulomb–franklin's algorithm, J. Inst. Eng. Ser. B 103 (2022) 1885–1908.
[7] A.S. Alghamdi, Optimal power flow of renewable-integrated power systems using a Gaussian bare- bones levy-flight firefly algorithm, Vol 10, Front. Energy Res. (2022).
[8] K. Gholami, A. Azizivahed, L. Li, J. Zhang, Accuracy enhancement of second-order cone relaxation for AC optimal power flow via linear mapping, Elec. Power Syst. Res. 212 (2022) 108646.
[9] S. Sarhan, R. El-Sehiemy, A. Abaza, M. Gafar, Turbulent flow of water-based optimization for solving multi-objective technical and economic aspects of optimal power flow problems, Mathematics 10 (2022) 2106.
[10] A.M. Shaheen, R.A. El-Sehiemy, H.M. Hasanien, A.R. Ginidi, An improved heap optimization algorithm for efficient energy management based optimal power flow model, Energy 250 (2022) 123795.
[11] H.T. Kahraman, M. Akbel, S. Duman, Optimization of optimal power flow problem using multi-objective manta ray foraging optimizer, Appl. Soft Comput. 116 (2022) 108334.
[12] M. Pourakbari-Kasmaei, J.R.S. Mantovani, Logically constrained optimal power flow: solver-based mixed-integer nonlinear programming model, Int. J. Electr. Power \& Energy Syst. 97 (2018) 240–249.
[13] J.A. Momoh, M.E. El-Hawary, R. Adapa, A review of selected optimal power flow literature to 1993. II. Newton, linear programming and interior point methods, IEEE Trans. Power Syst. 14 (1999) 105–111.
[14] M. Ghasemi, M. Zare, A. Zahedi, M.-A. Akbari, S. Mirjalili, L. Abualigah, Geyser inspired algorithm: a new geological-inspired meta-heuristic for real-parameter and constrained engineering optimization, J. Bionic Eng. (2023) 1–35.
[15] M. Ghasemi, M.-A. Akbari, C. Jun, S.M. Bateni, M. Zare, A. Zahedi, H.-T. Pai, S.S. Band, M. Moslehpour, K.-W. Chau, Circulatory System Based Optimization (CSBO): an expert multilevel biologically inspired meta-heuristic algorithm, Eng. Appl. Comput. Fluid Mech. 16 (2022) 1483–1525.
[16] I.U. Khan, N. Javaid, K.A.A. Gamage, C.J. Taylor, S. Baig, X. Ma, Heuristic algorithm based optimal power flow model incorporating stochastic renewable energy sources, IEEE Access 8 (2020) 148622–148643.
[17] K. Ayan, U. Kılıç, B. Baraklı, Chaotic artificial bee colony algorithm based solution of security and transient stability constrained optimal power flow, Int. J. Electr. Power Energy Syst. 64 (2015) 136–147, https://doi.org/10.1016/j.ijepes.2014.07.018.
[18] B. Ozkaya, S. Duman, H.T. Kahraman, U. Guvenc, Optimal solution of the combined heat and power economic dispatch problem by adaptive fitness-distance balance based artificial rabbits optimization algorithm, Expert Syst. Appl. 238 (2024) 122272.
[19] B. Mahdad, K. Srairi, T. Bouktir, Optimal power flow for large-scale power system with shunt FACTS using efficient parallel GA, Int. J. Electr. Power Energy Syst. 32 (2010) 507–517, https://doi.org/10.1016/j.ijepes.2009.09.013.
[20] A.A. El-Fergany, H.M. Hasanien, Single and multi-objective optimal power flow using grey wolf optimizer and differential evolution algorithms, Electr. Power Components Syst. 43 (2015) 1548–1559, https://doi.org/10.1080/15325008.2015.1041625.
[21] Z. Ullah, S. Wang, J. Radosavljević, J. Lai, A solution to the optimal power flow problem considering WT and PV generation, IEEE Access 7 (2019) 46763–46772.
[22] X. He, W. Wang, J. Jiang, L. Xu, An improved artificial bee colony algorithm and its application to multi-objective optimal power flow, Energies 8 (2015) 2412–2437, https://doi.org/10.3390/en8042412.
[23] M. Güçyetmez, E. Çam, A new hybrid algorithm with genetic-teaching learning optimization (G-TLBO) technique for optimizing of power flow in wind-thermal power systems, Electr. Eng. 98 (2016) 145–157.
[24] A. Khorsandi, S.H. Hosseinian, A. Ghazanfari, Modified artificial bee colony algorithm based on fuzzy multi-objective technique for optimal power flow problem, Electr. Power Syst. Res. 95 (2013) 206–213, https://doi.org/10.1016/j.epsr.2012.09.002.
[25] S. Surender Reddy, C. Srinivasa Rathnam, Optimal power flow using glowworm swarm optimization, Int. J. Electr. Power Energy Syst. 80 (2016) 128–139, https://doi.org/10.1016/j.ijepes.2016.01.036.
[26] H.T. Kahraman, S. Aras, E. Gedikli, Fitness-distance balance (FDB): a new selection method for meta-heuristic search algorithms, Knowledge-Based Syst. 190 (2020) 105169.
[27] U. Guvenc, S. Duman, H.T. Kahraman, S. Aras, M. Kat\i, Fitness–Distance Balance based adaptive guided differential evolution algorithm for security-constrained optimal power flow problem incorporating renewable energy sources, Appl. Soft Comput. 108 (2021) 107421.
[28] S. Duman, H.T. Kahraman, U. Guvenc, S. Aras, Development of a Lévy flight and FDB-based coyote optimization algorithm for global optimization and real-world ACOPF problems, Soft Comput 25 (2021) 6577–6617.
[29] R. Ma, X. Li, Y. Luo, X. Wu, F. Jiang, Multi-objective dynamic optimal power flow of wind integrated power systems considering demand response, CSEE J. Power Energy Syst. 5 (2019) 466–473.

[30] M.Z. Islam, N.I.A. Wahab, V. Veerasamy, H. Hizam, N.F. Mailah, J.M. Guerrero, M.N. Mohd Nasir, A Harris Hawks optimization based single-and multi-objective optimal power flow considering environmental emission, Sustainability 12 (2020) 5248.
[31] S. Duman, J. Li, L. Wu, U. Guvenc, Optimal power flow with stochastic wind power and FACTS devices: a modified hybrid PSOGSA with chaotic maps approach, Neural Comput. Appl. 32 (2020) 8463–8492, https://doi.org/10.1007/s00521-019-04338-y.
[32] Z.M. Ali, S.H.E.A. Aleem, A.I. Omar, B.S. Mahmoud, Economical-environmental-technical operation of power networks with high penetration of renewable energy systems using multi-objective coronavirus herd immunity algorithm, Mathematics 10 (2022) 1201.
[33] K. Dasgupta, P.K. Roy, V. Mukherjee, Power flow based hydro-thermal-wind scheduling of hybrid power system using sine cosine algorithm, Electr. Power Syst. Res. 178 (2020) 106018.
[34] A.-F. Attia, R.A. El Sehiemy, H.M. Hasanien, Optimal power flow solution in power systems using a novel Sine-Cosine algorithm, Int. J. Electr. Power Energy Syst. 99 (2018) 331–343, https://doi.org/10.1016/j.ijepes.2018.01.024.
[35] S. Mouassa, A. Althobaiti, F. Jurado, S.S.M. Ghoneim, Novel design of slim mould optimizer for the solution of optimal power flow problems incorporating intermittent sources: a case study of Algerian electricity grid, IEEE Access 10 (2022) 22646–22661.
[36] A. Maheshwari, Y.R. Sood, S. Jaiswal, S. Sharma, J. Kaur, Ant lion optimization based OPF solution incorporating wind turbines and carbon emissions, in: 2021 Innov. Power Adv. Comput. Technol., 2021, pp. 1–6.
[37] Sarda J., Pandya K., Lee K.Y., Hybrid cross entropy—cuckoo search algorithm for solving optimal power flow with renewable generators and controllable loads, Optim. Control Appl. Methods, Vol 44-2 , Page 508-532 (2021).
[38] M. Abdo, S. Kamel, M. Ebeed, J. Yu, F. Jurado, Solving non-smooth optimal power flow problems using a developed grey wolf optimizer, Energies 11 (2018) 1692.
[39] T. Niknam, M.R. Narimani, J. Aghaei, S. Tabatabaei, M. Nayeripour, Modified Honey Bee Mating Optimisation to solve dynamic optimal power flow considering generator constraints, IET Gener. Transm. Distrib. 5 (2011) 989, https://doi.org/10.1049/iet-gtd.2011.0055.
[40] T.T. Nguyen, A high performance social spider optimization algorithm for optimal power flow solution with single objective optimization, Energy 171 (2019) 218–240, https://doi.org/10.1016/j.energy.2019.01.021.
[41] R. Kyomugisha, C.M. Muriithi, G.N. Nyakoe, Performance of various voltage stability indices in a stochastic multiobjective optimal power flow using mayfly algorithm, J. Electr. Comput. Eng. 2022 (2022).
[42] M. Ahmad, N. Javaid, I.A. Niaz, A. Almogren, A. Radwan, A bio-inspired heuristic algorithm for solving optimal power flow problem in hybrid power system, IEEE Access 9 (2021) 159809–159826.
[43] A. Saha, A. Bhattacharya, P. Das, A.K. Chakraborty, A novel approach towards uncertainty modeling in multiobjective optimal power flow with renewable integration, Int. Trans. Electr. Energy Syst. 29 (2019) e12136, https://doi.org/10.1002/2050-7038.12136.
[44] N. Daryani, M.T. Hagh, S. Teimourzadeh, Adaptive group search optimization algorithm for multi-objective optimal power flow problem, Appl. Soft Comput. 38 (2016) 1012–1024, https://doi.org/10.1016/j.asoc.2015.10.057.
[45] A. Panda, M. Tripathy, A.K. Barisal, T. Prakash, A modified bacteria foraging based optimal power flow framework for Hydro-Thermal-Wind generation system in the presence of STATCOM, Energy 124 (2017) 720–740, https://doi.org/10.1016/j.energy.2017.02.090.
[46] L.H. Pham, B.H. Dinh, T.T. Nguyen, Optimal power flow for an integrated wind-solar-hydro-thermal power system considering uncertainty of wind speed and solar radiation, Neural Comput. Appl. (2022) 1–35.
[47] W. Warid, H. Hizam, N. Mariun, N. Abdul-Wahab, Optimal power flow using the Jaya algorithm, Energies 9 (2016) 678, https://doi.org/10.3390/en9090678.
[48] E.E. Elattar, S.K. ElSayed, Modified JAYA algorithm for optimal power flow incorporating renewable energy sources considering the cost, emission, power loss and voltage profile improvement, Energy 178 (2019) 598–609, https://doi.org/10.1016/j.energy.2019.04.159.
[49] H. Bakir, Optimal power flow analysis with circulatory system-based optimization algorithm, Turkish J. Eng. 8 (n.d.) 92–106.
[50] M. Ghasemi, P. Trojovsk\'y, E. Trojovská, M. Zare, Gaussian bare-bones Levy circulatory system-based optimization for power flow in the presence of renewable units, Eng. Sci. Technol. an Int. J. 47 (2023) 101551.
[51] L. Shi, C. Wang, L. Yao, Y. Ni, M. Bazargan, Optimal power flow solution incorporating wind power, IEEE Syst. J. 6 (2011) 233–241.
[52] S.R. Salkuti, Optimal power flow using multi-objective glowworm swarm optimization algorithm in a wind energy integrated power system, Int. J. Green Energy 16 (2019) 1547–1561, https://doi.org/10.1080/15435075.2019.1677234.
[53] M. Riaz, A. Hanif, S.J. Hussain, M.I. Memon, M.U. Ali, A. Zafar, An optimization-based strategy for solving optimal power flow problems in a power system integrated with stochastic solar and wind power energy, Appl. Sci. 11 (2021) 6883.
[54] R. Kyomugisha, C.M. Muriithi, M. Edimu, Multiobjective optimal power flow for static voltage stability margin improvement, Heliyon 7 (2021) e08631.
[55] M. Basu, Multi-objective optimal power flow with FACTS devices, Energy Convers. Manag. 52 (2011) 903–910, https://doi.org/10.1016/j.enconman.2010.08.017.
[56] M. Varadarajan, K.S. Swarup, Solving multi-objective optimal power flow using differential evolution, IET Gener. Transm. Distrib. 2 (2008) 720, https://doi.org/10.1049/iet-gtd:20070457.
[57] M. Ghasemi, M. Zare, S.K. Mohammadi, S. Mirjalili, Applications of whale migration algorithm in optimal power flow problems of power systems, in: Handb. Whale Optim. Algorithm, Elsevier, 2024, pp. 347–364.
[58] M. Ghasemi, S. Ghavidel, J. Aghaei, M. Gitizadeh, H. Falah, Application of chaos-based chaotic invasive weed optimization techniques for environmental OPF problems in the power system, Chaos, Solitons and Fractals 69 (2014), https://doi.org/10.1016/j.chaos.2014.10.007.
[59] Avvari R.K., DM V.K., A novel hybrid multi-objective evolutionary algorithm for optimal Power flow in wind, PV, and PEV systems, J. Oper. Autom. Power Eng., Vol 11- 2, Page 130 - 143 (2022).
[60] K. Teeparthi, D.M. Vinod Kumar, Multi-objective hybrid PSO-APO algorithm based security constrained optimal power flow with wind and thermal generators, Eng. Sci. Technol. an Int. J. 20 (2017) 411–426, https://doi.org/10.1016/j.jestch.2017.03.002.
[61] X. Yuan, B. Zhang, P. Wang, J. Liang, Y. Yuan, Y. Huang, X. Lei, Multi-objective optimal power flow based on improved strength Pareto evolutionary algorithm, Energy 122 (2017) 70–82, https://doi.org/10.1016/j.energy.2017.01.071.
[62] M.H. Hassan, S.K. Elsayed, S. Kamel, C. Rahmann, I.B.M. Taha, Developing chaotic Bonobo optimizer for optimal power flow analysis considering stochastic renewable energy resources, Int. J. Energy Res. 46 (8) (2022) 11291–11325.
[63] E.E. Elattar, Optimal power flow of a power system incorporating stochastic wind power based on modified moth swarm algorithm, IEEE Access 7 (2019) 89581–89593.
[64] B. Venkateswara Rao, G.V. Nagesh Kumar, Optimal power flow by BAT search algorithm for generation reallocation with unified power flow controller, Int. J. Electr. Power Energy Syst. 68 (2015) 81–88, https://doi.org/10.1016/j.ijepes.2014.12.057.
[65] B. Jeddi, A.H. Einaddin, R. Kazemzadeh, Optimal power flow problem considering the cost, loss, and emission by multi-objective electromagnetism-like algorithm, 2016 6th Conf. Therm. Power Plants (2016), https://doi.org/10.1109/ctpp.2016.7482931.
[66] S. Duman, S. Rivera, J. Li, L. Wu, Optimal power flow of power systems with controllable wind-photovoltaic energy systems via differential evolutionary particle swarm optimization, Int. Trans. Electr. Energy Syst. 30 (2020) e12270, https://doi.org/10.1002/2050-7038.12270.
[67] S. Chandrasekaran, Multiobjective optimal power flow using interior search algorithm: a case study on a real-time electrical network, Comput. Intell. 36 (2020) 1078–1096, https://doi.org/10.1111/coin.12312.
[68] C. Srithapon, P. Fuangfoo, P.K. Ghosh, A. Siritaratiwat, R. Chatthaworn, Surrogate-Assisted multi-objective probabilistic optimal power flow for distribution network with photovoltaic generation and electric vehicles, IEEE Access 9 (2021) 34395–34414.
[69] B.A. Kumari, K. Vaisakh, Integration of solar and flexible resources into expected security cost with dynamic optimal power flow problem using a Novel DE algorithm, Renew. Energy Focus, Vol 42, Page 48-69 (2022).
[70] H.R.E.H. Bouchekara, A.E. Chaib, M.A. Abido, R.A. El-Sehiemy, Optimal power flow using an improved colliding Bodies optimization algorithm, Appl. Soft Comput. 42 (2016) 119–131, https://doi.org/10.1016/j.asoc.2016.01.041.

[71] O. Herbadji, L. Slimani, T. Bouktir, Optimal power flow with four conflicting objective functions using multiobjective ant lion algorithm: a case study of the algerian electrical network, Iran, J. Electr. Electron. Eng. 15 (2019) 94–113, https://doi.org/10.22068/IJEEE.15.1.94.

[72] S. Li, W. Gong, L. Wang, X. Yan, C. Hu, Optimal power flow by means of improved adaptive differential evolution, Energy 198 (2020) 117314, https://doi.org/10.1016/j.energy.2020.117314.

[73] S. Duman, J. Li, L. Wu, AC optimal power flow with thermal–wind–solar–tidal systems using the symbiotic organisms search algorithm, IET Renew. Power Gener. 15 (2021) 278–296.

[74] R. Rajabioun, Cuckoo optimization algorithm, Appl. Soft Comput. 11 (2011) 5508–5518.

[75] S.A. Moezi, E. Zakeri, A. Zare, M. Nedaei, On the application of modified cuckoo optimization algorithm to the crack detection problem of cantilever Euler–Bernoulli beam, Comput. \& Struct. 157 (2015) 42–50.

[76] M. Mehdinejad, B. Mohammadi-Ivatloo, R. Dadashzadeh-Bonab, Energy production cost minimization in a combined heat and power generation systems using cuckoo optimization algorithm, Energy Effic 10 (2017) 81–96.

[77] E. Amiri, S. Mahmoudi, Efficient protocol for data clustering by fuzzy cuckoo optimization algorithm, Appl. Soft Comput. 41 (2016) 15–21.

[78] M. Yakhchi, S.M. Ghafari, S. Yakhchi, M. Fazeli, A. Patooghi, Proposing a load balancing method based on Cuckoo Optimization Algorithm for energy management in cloud computing infrastructures, in: 2015 6th Int. Conf. Model. Simulation, Appl. Optim., 2015, pp. 1–5.

[79] A.S. Alghamdi, A hybrid firefly–JAYA algorithm for the optimal power flow problem considering wind and solar power generations, Appl. Sci. 12 (2022) 7193.

[80] M. Ghasemi, A chaotic modified algorithm for economic dispatch problems with generator constraints, Am. J. Electr. Comput. Eng. 1 (2017) 61–71.

[81] S. Kamel, M. Ebeed, F. Jurado, An improved version of salp swarm algorithm for solving optimal power flow problem, Soft Comput 25 (2021) 4027–4052.

[82] S. Duman, L. Wu, J. Li, Moth swarm algorithm based approach for the ACOPF considering wind and tidal energy, in: Int. Conf. Artif. Intell. Appl. Math. Eng., Springer, 2019, pp. 830–843.

[83] P.P. Biswas, P.N. Suganthan, G.A.J. Amaratunga, Optimal power flow solutions incorporating stochastic wind and solar power, Energy Convers. Manag. 148 (2017) 1194–1207.

[84] S. Duman, H.T. Kahraman, B. Korkmaz, H. Bakir, U. Guvenc, C. Yilmaz, Improved phasor particle swarm optimization with fitness distance balance for optimal power flow problem of hybrid AC/DC power grids, in: Int. Conf. Artif. Intell. Appl. Math. Eng, 2021, pp. 307–336.

[85] Y. Sonmez, S. Duman, H.T. Kahraman, M. Kati, S. Aras, U. Guvenc, Fitness-distance balance based artificial ecosystem optimisation to solve transient stability constrained optimal power flow problem, J. Exp. \& Theor. Artif. Intell. (2022) 1–40.

[86] M. Ghasemi, M. Zare, A. Zahedi, P. Trojovsk\'y, L. Abualigah, E. Trojovská, Optimization based on performance of lungs in body: lungs performance-based optimization (LPO), Comput. Methods Appl. Mech. Eng. 419 (2024) 116582.

[87] A.W. Moore, Clustering with Gaussian mixtures, Sch. Comput. Sci. Carnegie Mellon Univ. (2001).

[88] D.A. Reynolds, others, Gaussian mixture models, Encycl. Biometrics 741 (2009).

[89] N. Shental, A. Bar-Hillel, T. Hertz, D. Weinshall, Computing Gaussian mixture models with EM using equivalence constraints, Adv. Neural Inf. Process. Syst. 16 (2003).

[90] H.T. Kahraman, M. Kat\i, S. Aras, D.A. Ta\csci, Development of the Natural Survivor Method (NSM) for designing an updating mechanism in metaheuristic search algorithms, Eng. Appl. Artif. Intell. 122 (2023) 106121.

[91] B. Ozkaya, H.T. Kahraman, S. Duman, U. Guvenc, Fitness-Distance-Constraint (FDC) based guide selection method for constrained optimization problems, Appl. Soft Comput. 144 (2023) 110479.

[92] H.T. Kahraman, M.H. Hassan, M. Kat\i, M. Tostado-Véliz, S. Duman, S. Kamel, Dynamic-fitness-distance-balance stochastic fractal search (dFDB-SFS algorithm): an effective metaheuristic for global optimization and accurate photovoltaic modeling, Soft Comput (2023) 1–28.

[93] R.D. Zimmerman, C.E. Murillo-Sánchez, R.J. Thomas, MATPOWER: steady-state operations, planning, and analysis tools for power systems research and education, IEEE Trans. Power Syst. 26 (2010) 12–19.

[94] M. Ghasemi, Modified Imperialist Competitive Algorithm for Optimal Reactive Power Dispatch, (n.d.).

[95] H.R.E.H. Bouchekara, A.E. Chaib, M.A. Abido, R.A. El-Sehiemy, Optimal power flow using an improved colliding Bodies optimization algorithm, Appl. Soft Comput. 42 (2016) 119–131.

[96] M. Ghasemi, S. Ghavidel, M.M. Ghanbarian, A. Habibi, A new hybrid algorithm for optimal reactive power dispatch problem with discrete and continuous control variables, Appl. Soft Comput. J. 22 (2014), https://doi.org/10.1016/j.asoc.2014.05.006.

[97] M. Ghasemi, M.M. Ghanbarian, S. Ghavidel, S. Rahmani, E. Mahboubi Moghaddam, Modified teaching learning algorithm and double differential evolution algorithm for optimal reactive power dispatch problem: a comparative study, Inf. Sci. (Ny). 278 (2014), https://doi.org/10.1016/j.ins.2014.03.050.

[98] M. Ghasemi, S. Ghavidel, S. Rahmani, A. Roosta, H. Falah, A novel hybrid algorithm of imperialist competitive algorithm and teaching learning algorithm for optimal power flow problem with non-smooth cost functions, Eng. Appl. Artif. Intell. 29 (2014) 54–69, https://doi.org/10.1016/j.engappai.2013.11.003.

[99] Y. Sood, Evolutionary programming based optimal power flow and its validation for deregulated power system analysis, Int. J. Electr. Power Energy Syst. 29 (2007) 65–75, https://doi.org/10.1016/j.ijepes.2006.03.024.

[100] H. Pulluri, R. Naresh, V. Sharma, A solution network based on stud krill herd algorithm for optimal power flow problems, Soft Comput 22 (2018) 159–176, https://doi.org/10.1007/s00500-016-2319-3.

[101] A. Ramesh Kumar, L. Premalatha, Optimal power flow for a deregulated power system using adaptive real coded biogeography-based optimization, Int. J. Electr. Power Energy Syst. 73 (2015) 393–399, https://doi.org/10.1016/j.ijepes.2015.05.011.

[102] W. Ongsakul, T. Tantimaporn, Optimal power flow by improved evolutionary programming, Electr. Power Components Syst. 34 (2006) 79–95, https://doi.org/10.1080/15325000691001458.

[103] A.K. Khamees, A.Y. Abdelaziz, M.R. Eskaros, A. El-Shahat, M.A. Attia, Optimal power flow solution of wind-integrated power system using novel metaheuristic method, Energies 14 (2021) 6117.

[104] A.-A.A. Mohamed, Y.S. Mohamed, A.A.M. El-Gaafary, A.M. Hemeida, Optimal power flow using moth swarm algorithm, Electr. Power Syst. Res. 142 (2017) 190–206, https://doi.org/10.1016/j.epsr.2016.09.025.

[105] K. Abaci, V. Yamacli, Differential search algorithm for solving multi-objective optimal power flow problem, Int. J. Electr. Power Energy Syst. 79 (2016) 1–10, https://doi.org/10.1016/j.ijepes.2015.12.021.

[106] M.A. Abido, Optimal power flow using tabu search algorithm, Electr. Power Components Syst. 30 (2002) 469–483, https://doi.org/10.1080/15325000252888425.

[107] M. Ghasemi, S. Ghavidel, M.M. Ghanbarian, M. Gitizadeh, Multi-objective optimal electric power planning in the power system using Gaussian bare-bones imperialist competitive algorithm, Inf. Sci. (Ny) (2015) 294, https://doi.org/10.1016/j.ins.2014.09.051.

[108] J. Radosavljević, D. Klimenta, M. Jevtić, N. Arsić, Optimal power flow using a hybrid optimization algorithm of particle swarm optimization and gravitational search algorithm, Electr. Power Components Syst. 43 (2015) 1958–1970, https://doi.org/10.1080/15325008.2015.1061620.

[109] S. Sayah, K. Zehar, Modified differential evolution algorithm for optimal power flow with non-smooth cost functions, Energy Convers. Manag. 49 (2008) 3036–3042, https://doi.org/10.1016/j.enconman.2008.06.014.

[110] U. Guvenc, H. Bakir, S. Duman, B. Ozkaya, Optimal power flow using manta ray foraging optimization, in: Int. Conf. Artif. Intell. Appl. Math. Eng., 2020, pp. 136–149.

[111] R. Roy, H.T. Jadhav, Optimal power flow solution of power system incorporating stochastic wind power using Gbest guided artificial bee colony algorithm, Int. J. Electr. Power Energy Syst. 64 (2015) 562–578, https://doi.org/10.1016/j.ijepes.2014.07.010.

[112] L. Jebaraj, S. Sakthivel, A new swarm intelligence optimization approach to solve power flow optimization problem incorporating conflicting and fuel cost based objective functions, E-Prime-Advances Electr. Eng. Electron, Energy 2 (2022) 100031.

[113] P.P. Biswas, P.N. Suganthan, R. Mallipeddi, G.A.J. Amaratunga, Optimal power flow solutions using differential evolution algorithm integrated with effective constraint handling techniques, Eng. Appl. Artif. Intell. 68 (2018) 81–100, https://doi.org/10.1016/j.engappai.2017.10.019.

[114] W. Warid, H. Hizam, N. Mariun, N.I. Abdul Wahab, A novel quasi-oppositional modified Jaya algorithm for multi-objective optimal power flow solution, Appl. Soft Comput. 65 (2018) 360–373, https://doi.org/10.1016/j.asoc.2018.01.039.
[115] B. Bentouati, A. Khelifi, A.M. Shaheen, R.A. El-Sehiemy, An enhanced moth-swarm algorithm for efficient energy management based multi dimensions OPF problem, J. Ambient Intell. Humaniz. Comput (2020) 1–21, https://doi.org/10.1007/s12652-020-02692-7.
[116] M. Ghasemi, S. Ghavidel, M.M. Ghanbarian, M. Gharibzadeh, A. Azizi Vahed, Multi-objective optimal power flow considering the cost, emission, voltage deviation and power losses using multi-objective modified imperialist competitive algorithm, Energy 78 (2014) 276–289, https://doi.org/10.1016/j.energy.2014.10.007.
[117] S. Gupta, N. Kumar, L. Srivastava, H. Malik, A. Pliego Marugán, F.P. Garc\'\ia Márquez, A hybrid Jaya–powell's pattern search algorithm for multi-objective optimal power flow incorporating distributed generation, Energies 14 (2021) 2831.
[118] R.A. El Sehiemy, F. Selim, B. Bentouati, M.A. Abido, A novel multi-objective hybrid particle swarm and salp optimization algorithm for technical-economical-environmental operation in power systems, Energy 193 (2020) 116817.
[119] A. Meng, C. Zeng, P. Wang, D. Chen, T. Zhou, X. Zheng, H. Yin, A high-performance crisscross search based grey wolf optimizer for solving optimal power flow problem, Energy 225 (2021) 120211.
[120] M.H. Hassan, S. Kamel, A. Selim, T. Khurshaid, J.L. Domínguez-García, A modified Rao-2 algorithm for optimal power flow incorporating renewable energy sources, Mathematics 9 (2021) 1532.
[121] J. Derrac, S. Garc\'\ia, D. Molina, F. Herrera, A practical tutorial on the use of nonparametric statistical tests as a methodology for comparing evolutionary and swarm intelligence algorithms, Swarm Evol. Comput. 1 (2011) 3–18.
[122] S. Gürgen, H.T. Kahraman, S. Aras, Ismail Alt\in, A comprehensive performance analysis of meta-heuristic optimization techniques for effective organic rankine cycle design, Appl. Therm. Eng. 213 (2022) 118687.
[123] H.T. Öztürk, H.T. Kahraman, Meta-heuristic search algorithms in truss optimization: research on stability and complexity analyses, Appl. Soft Comput. 145 (2023) 110573.